YEDITEPE UNIVERSITY
GRADUATE SCHOOL OF NATURAL AND APPLIED SCIENCES

DETERMINATION THE EFFECTS OF IL-6 CYTOKINE PATHWAY ON THE CHORDOMA PATHOPHYSIOLOGY

A Dissertation Submitted
by
Melike Bayındır Bilgiç

In Partial Fulfillment
of the Requirements for the Degree of
Doctor of Philosophy
in
Biotechnology

Supervisor
Prof. Dr. Ömer Faruk Bayrak

Istanbul - 2024

DETERMINATION THE EFFECTS OF IL-6 CYTOKINE PATHWAY ON THE CHORDOMA PATHOPHYSIOLOGY

by

Melike Bayındır Bilgiç

Approved by:

Prof. Dr. Ömer Faruk Bayrak
(Yeditepe University) .....
(Thesis Supervisor)

Prof. Dr. Dilek Telci Temeltaş
(Yeditepe University) .....

Prof. Dr. Şükrü Öztürk
(Istanbul University) .....

Assoc. Prof. Dr. Ayşegül Kuşkucu
(Yeditepe University) .....

Assist. Prof. Dr. Şükrü Güllüoğlu
(Marmara University) .....

DATE OF APPROVAL: ..../..../20...

DECLARATION OF ORIGINALITY

I hereby declare that this thesis is my own work and that all information in this thesis has been obtained and presented following academic rules and ethical conduct. I have fully cited and referenced all material and results as required by these rules and conduct, and this thesis study does not contain any plagiarism. The necessary permissions have been obtained if any material used in the thesis requires copyright. No material from this thesis has been used to award another degree.

To the best of my knowledge and belief, it contains no material previously published or written by another person nor material accepted for the award of any other degree except where due acknowledgment has been made in the text.

I accept all kinds of legal liability that may arise in cases contrary to these situations.

Melike Bayındır Bilgiç

Signature

ABSTRACT

DETERMINATION THE EFFECTS OF THE IL-6 CYTOKINE PATHWAY ON THE CHORDOMA PATHOPHYSIOLOGY

Chordomas are rare aggressive primary bone tumors affecting the skull base and spine. Given the limited options available to prevent and treat progression, there remains an urgent need to develop novel therapies to improve clinical outcomes.

IL-6 is a potent, pleiotropic, inflammatory cytokine that involved in cell proliferation and differentiation. Although IL-6 signaling has been investigated in many cancers, its function in chordoma has not yet been elucidated. This study investigated the effects of the IL-6 signaling pathway on chordomas, which has been found to affect carcinogenesis in other types of cancer directly.

The IL-6 receptor was targeted using CRISPR/Cas9-mediated knock-out, shRNA-mediated knock-down, and Tocilizumab-mediated inhibition in two different chordoma cell lines. Among these methods, the shRNA-mediated strategy was efficient to generate IL-6R silenced chordoma cell lines. Accordingly, stable IL-6R silenced JHC7 and MUG-Chor1 cell lines were generated. The functional effects of IL-6R silencing on chordomas were investigated by evaluating invasion, migration, CSC, EMT, and sphere-formation abilities. By performing whole transcriptome analysis, differentially expressed genes and related pathways in IL-6R silenced cells were identified. The findings indicated that IL-6 signaling promotes aggressiveness in chordomas, and silencing IL-6R reduced invasion and migration capacities of these cells. Functional enrichment analyses identified pathways and genes affected in IL-6R silenced chordomas compared to control cells, revealing 3 increased and 2 decreased candidate genes. Additionally, analysis with the DAVID database showed a significant increase in the expression of the Hippo signaling pathway in both cell lines upon silencing IL-6R expression.

In conclusion, this dissertation contributes to the identification of potential candidate genes and pathways by conducting a functional and transcriptomic investigation of the IL-6 signaling pathway in chordoma.

ÖZET

IL-6 SİTOKİN YOLAĞININ KORDOMA PATOFİZYOLOJİSİ ÜZERİNDEKİ ETKİLERİNİN BELİRLENMESİ

Kordomalar, kafa tabanı ve omurgayı etkileyen nadir agresif primer kemik tümörleridir. Progresyonu önlemek ve tedavi etmek için mevcut sınırlı seçenekler göz önüne alındığında, yeni tedavilerin geliştirilmesine ihtiyaç vardır.

İnterlökin-6, hücre proliferasyonu/farklılaşması sürecine katılan güçlü, pleiotropik, inflamatuar bir sitokindir. IL-6 sinyalizasyonunun birçok kanser üzerinde araştırılmasına rağmen kordomadaki işlevi henüz aydınlatılamamıştır. Bu çalışmada, diğer kanser türlerinde karsinogenezi doğrudan etkilediği tespit edilen IL-6 sinyal yolağının kordomalar üzerindeki etkileri araştırılmıştır.

Reseptörün hedeflenmesi için CRISPR/Cas9 aracılı silme, shRNA aracılı susturma ve Tocilizumab aracılı inhibisyon yöntemleri kullanılmıştır. Bu yöntemler arasından shRNA aracılı strateji, stabil IL-6R susturulmuş JHC7 ve MUG-Chor1 hücre hatları oluşturmak için etkili olmuştur. Susturulmuş IL-6R ifadesinin kordomalar üzerindeki fonksiyonel etkisini belirlemek üzere invazyon, göç, CSC ve EMT kapasitesi ve küre oluşturma potansiyeli incelenmiştir. Tüm transkriptom analizi yapılarak, IL-6R susturulmuş hücrelerde diferansiyel olarak ifade edilen genler ve ilgili yolaklar tanımlanmıştır. Bulgular IL-6 sinyalinin kordomalarda agresifliği desteklediğini ve IL-6R'nin susturulmasının bu hücrelerin invazyon ve migrasyon kapasitelerini azalttığını göstermiştir. Fonksiyonel zenginleştirme analizleri, kontrol hücrelerine kıyasla IL-6R susturulmuş kordomalarda etkilenen yolakları ve genleri tanımlamış, 3 artmış ve 2 azalmış aday gen ortaya çıkarmıştır. Ek olarak, DAVID veri tabanı ile yapılan analiz, IL-6R ekspresyonunun susturulması üzerine her iki hücre hattında da Hippo sinyal yolunun ekspresyonunda önemli bir artış olduğunu göstermiştir.

Bu tez çalışması, kordomada IL-6 sinyal yolağının işlevsel ve transkriptomik bir araştırmasını yaparak potansiyel aday genlerin ve yolakların tanımlanmasına katkıda bulunmaktadır.

ACKNOWLEDGEMENTS

I would like to extend sincere appreciation to all the people and organizations that helped me finish my doctoral dissertation.

First and foremost, I would like to thank my advisor, Prof. Dr. Ömer Faruk BAYRAK, for constant guidance, invaluable suggestions, and patience. Prof. Dr. Ömer Faruk BAYRAK, expertise and experience have played a critical role in the development of this thesis. I am appreciative of him for being a significant role model in my academic career and for making me feel like I was family.

I would like to express my gratitude to dear Dr. Nur EKİMCİ GÜRCAN for her valuable friendship and all academic support. I am grateful to my dear lab mates MSc. Didem TECİMEL, Dr. Didem SEVEN, MSc. Berfin UZUNKAYA, MSc. Gizem İNETAŞ YENGİN, Dr. Utku ÖZBEY, and Dr. Emre Can TÜYSÜZ for their support throughout my PhD journey.

My team members who accompanied all my humorousness in my Ph.D. process and provided me with a joyful academic environment were Dr. Negar TAGHAVI POURIANAZAR, MSc. Mesut ŞAHİN, Ebru BAKTEMUR, Dr. Öznur SUAKAR, MSc. Sezin GÜRKAN and of course my beloved advisor Assoc. Prof. Dr. Ayşegül, KUŞKUCU.

I would like to extend my thanks to my family for supporting me throughout the thesis process. And of course, I am grateful to my dear son Ömer BİLGİÇ, a junior member of my family, for his endless love despite my sleepless nights. Finally, I would like to thank my dear spouse Selim BİLGİÇ. Without his tremendous support and encouragement, it would have been impossible for me to complete this journey.

I would like to thank TÜBİTAK for their contribution to the scholarship that I received as a TÜBİTAK BİDEB 2211-A scholar.

This work was supported by the Scientific and Technological Research Council of Turkey [Grant number 222S197].

TABLE OF CONTENTS

LIST OF FIGURES

LIST OF TABLES

LIST OF ABBREVIATIONS

USA	United States of America
SEER	Surveillance, Epidemiology, and End Results
CT	Computerized Tomography
MRI	Magnetic Resonance Imaging
FBS	Fetal Bovine Serum
PS	Penicillin-Streptomycin
IMDM	Iscove's Modified Dulbecco's Medium
RPMI	Roswell Park Memorial Institute
TBXT	T-box transcription factor protein
TME	Tumor microenvironment
ECM	Extracellular matrix
NKT2	Natural killer-T Type-2
shRNA	Short hairpin RNA
siRNA	Small interfering RNA
RISC	RNA-induced silencing complex
RNAi	RNA interference
NHEJ	Non-homologous end-joining
HDR	Homology-directed repair
CRISPR	Clustered Regularly Interspaced Short Palindromic Repeats
DSB	Double-strand break
cDNA	Complementary DNA
qRT-PCR	Quantitative Real-Time Polymerase Chain Reaction
BCA	Bicinchoninic acid
RIPA	Radioimmunoprecipitation Assay
HRP	Horseradish peroxidase
JAK	Janus Kinase
STAT	Signal transducer and activator of transcription
MAPK	A mitogen-activated protein kinase
TAM	Tumor-associated macrophages

1. INTRODUCTION

Cancer is a disease characterized by uncontrolled cell divisions resulting from molecular alterations, primarily stemming from the accumulation of mutations in previously healthy cells. Once these cells undergo such changes, they are referred to as "cancer cells," and their proliferation becomes responsible for the development of tumors. The progression and initiation of cancer constitute a complex, multi-step process, influenced by environmental factors, genetic components, and disturbances in molecular mechanisms. [1, 5].

Cancers are divided into classes according to the type of cell and tissue from which they originate. Carcinomas are cancers originating from epithelial cells and are the most common type of cancer in humans. In addition, epithelial tissues are most likely to be exposed to various physical and chemical damages that promote cancer development. Sarcomas are caused by muscle or connective tissue cells. Apart from these two types of cancer, there are also leukemias, lymphomas, and cancers originating from nervous system cells.

Multiple types of cell populations surround the cancer cells, and these cells have the potential to affect adjacent normal cells, compounds, and blood vessels. This region is known as the tumor microenvironment, characterized by a diverse collection of cell groups. The most important elements of the tumor microenvironment are the extracellular matrix, infiltrating cells, and inflammatory molecules. The components of the tumor microenvironment play a crucial role in guiding the course of the tumor by directing the signals essential for its growth and development [1]. Cancer cells can affect the normal cells, molecules, and blood vessels that surround and feed a tumor. Cancer cells can often evade the immune system which has organs, tissues, and other specialized cells that protect the body from infections and other conditions. Even though the immune system ordinarily removes abnormal or damaged cells from the body, some cancer cells can hide from the immune system. Tumor cells are also able to use the immune system to survive and grow [1, 3].

Cytokines are among the components of the tumor microenvironment that possesses the ability to directly impact the defence mechanisms of the immune system. The effects of cytokines on tumor progression are controversial. Cytokines, one of the mediators of the relationship between tumor and immune system defence, is an important target that needs to be investigated for chordoma [2].

Certain members of the cytokine family, due to their pleitropic properties, either enhance the immune response or promote carcinogenesis. The mechanism underlying this critical response of cytokines has not yet been fully elucidated [3, 4]. The interleukin-6 (IL-6) is a robust, pleiotropic, inflammatory cytokine. Considering its pro-inflammatory and anti-inflammatory properties, IL-6 is an important molecule for determining the progression of cancer.

Understanding the complex interaction between cancer and cytokines is crucial for the development of novel therapeutic strategies targeting the tumor microenvironment. Harnessing the immunomodulatory properties of cytokines holds promise for the development of immunotherapies that focus on enhancing anti-tumor immune responses and overcoming immune evasion mechanisms used by cancer cells.

2. THEORETICAL BACKGROUND

Cancer is characterized by the uncontrolled growth and spread of abnormal cells. These cells are able to evade cell control mechanisms and expand to become tumors. The cancer cells that generate the tumor are able to infiltrate into neighboring tissues and organs and disrupt their normal physiological processes. Progression and initiation of cancer is a multistep process. Genetic factors and corruption of molecular mechanisms take part together with environmental factors. Cancer development and progression are influenced not only by intrinsic genetic alterations within cancer cells but also by interactions with the tumor microenvironment. The extracellular matrix, immune cells, stromal cells, blood vessels, and signaling molecules like growth factors and cytokines are all parts of the tumor microenvironment. Immune evasion, tumor development, invasion, and metastasis are all significantly aided by crosstalk between cancer cells and the microenvironment.

Determination of molecular pathways and proteins that are responsible for carcinogenesis is a very important part of cancer treatment. It is required to better understand the chordoma progression mechanisms, which are still unclear. Chordoma, an exceptionally uncommon form of cancer, lacks sufficient elucidation in the existing literature and requires further exploration and understanding.

2.1. MALIGNANT BONE TUMORS

Malignant bone tumors represent a small percentage of cancers. The rarity of this type of cancer makes it difficult to identify evidence pointing to a potential bone malignancy. The scarcity of this cancer type adds complexity to the identification of signs indicative of a potential bone malignancy. Osteosarcoma and Ewing's sarcoma are the two most prevalent primary malignant bone tumors, that occur in childhood. Chondrosarcoma is more common in older people. Rare malignant bone tumors such as chordoma are more commonly localized in the clivus or sacrum [5, 6].

Malignant bone tumors are extremely difficult to avoid and diagnose in their early stages. Therefore, it requires comprehensive interventions including creating resources for early detection/screening and increasing awareness of rare cancers [5].

There are ongoing attempts to expand knowledge and establish novel approaches to therapy in this field. Among these initiatives include the development of gene therapy, immunotherapy, targeted therapies, and other cutting-edge medical procedures. Malignant bone cancer is still an important health problem that has to be handled with ongoing research and improved treatment options.

2.1.1. CHORDOMA

Chordoma is a rare bone malignancy of notochord origin that affects the axial skeleton. The notochord, a structure that exists in human embryos, is the precursor of the spinal cord. This structure disappears before birth, in some cases, these cells remain in the spine or at the base of the skull. These notochord cells are responsible for the development of a chordoma, but the exact mechanism is unclear [6, 8].

Chordomas are also aggressive tumors that can originate anywhere along the spine although most commonly in the clivus or sacrum. Chordomas have high local and distal recurrence rates, with a 5-year survival rate of 73%-86% and a 10-year survival rate of 49%-71%. According to Surveillance, Epidemiology, and End Results (SEER) data, the incidence of chordoma in the USA is 1 per million and the 5-year survival rate is approximately 80.3%. Although chordoma can occur in people of any age or gender, it is most frequently diagnosed in adults between the ages of 40 and 70. It was discovered that there was a 1.8:1 incidence rate between males and females [8, 10].

Chordomas are able to be classified into three different categories by the World Health Organization (WHO): poorly differentiated chordomas, dedifferentiated chordomas, and conventional chordomas. All three forms of tumors are malignant and have a significant risk of metastasis and local recurrence. The dedifferentiated chordoma type has a poor prognosis and the highest metastasis rate [7, 8]. Although chordomas are regarded as non-anaplastic tumors, dedifferentiated chordomas are anaplastic. Certain keratins (CK8, CK18, CK19), epithelial membrane antigen (EMA), nuclear brachyury (TBXT), S-100, vimentin, and epithelial membrane antigen all stain positively in chordoma and negative for CK7 and CK20 [7, 9].

The most frequent initial complaints of chordoma patients are pain and neurological problems because of their localization. Clinically, pathological diagnostic approaches based

on immunohistochemistry and non-invasive imaging techniques are used to diagnose chordomas [10]. Imaging techniques such as CT scans, X-rays, or MRI scans are frequently used in diagnosis to determine the location and size of the tumor. A biopsy may be performed to confirm the presence of a chordoma. The prognosis of chordoma depends on factors such as the size and location of the tumor and whether it has spread to other parts of the body. Although chordomas usually expand slowly, they can occasionally be locally aggressive and recur even after treatment [8, 9].

A hallmark of chordoma is the expression of T-box transcription factor protein (TBXT), which encodes the developmentally regulated transcription factor *Brachyury*. *Brachyury* is a potential therapeutic target and a main driver of chordoma cell proliferation and pathogenesis, in addition to being a diagnostic biomarker for the disease [11]. At the embryonic stage, *Brachyury* is crucial for the development of the notochord into the axial skeleton and bone. Therefore, the high expression of *Brachyury* in chordomas is the basis for the hypothesis that chordomas develop from embryonic notochord remains. Detection of *Brachyury* overexpression is often used as a diagnostic marker to confirm the presence of chordoma as it is specific to this type of cancer [12, 13].

Chordoma is a rare bone tumor with a 5-year recurrence-free survival rate of 50% despite aggressive treatment, making chordoma a therapeutic challenge. The main treatment approach for chordoma is total bloc resection. In addition, radiation therapy is also preferred to support the surgical operation. Besides surgical resection and radiation therapy methods, there are no approved systemic therapies for chordoma patients with unresectable or metastatic tumors. Given the limited options to prevent and treat chordoma progression, the necessity for finding novel treatments remains. Due to its rarity, it is challenging to create chordoma cohorts that allowing extensive biological and molecular investigations. Therefore, it is necessary to understand the biology of chordoma, genetic factors and molecular alterations, as well as the interactions between chordoma and the immune tumor microenvironment (IME) [14].

2.2. TUMOR MICROENVIRONMENT

Research studies on the tumor phenomenon have demonstrated that a tumor is not a collection of abnormal cells, but a much more organized structure. The tumor

microenvironment (TME), which is composed of several various components that constitute cancers, varies depending on the type of tumor [15, 16]. In general, the main elements that composed of the TME are tumor cells, immune cells, stromal cells, extracellular matrix (ECM), vessels, soluble factors, and physical properties [1]. Solid tumors contain neoplastic and non-neoplastic stromal cells embedded in a dynamic ECM microenvironment. During the early stages of tumor development, a dynamic and reciprocal connection forms between cancer cells and factors of the tumor microenvironment, promoting cancer cell survival, local invasion, and metastatic growth [15]. Immune cells are critical components of the tumor microenvironment. The balance between pro- and anti-tumor inflammatory mediators can affect tumor progression. Tumors can gradually transform the tumor immune microenvironment (TIME) into an immunosuppressive state to resist the host's immunity [17].

According to Steven Paget's "seed and soil" hypothesis, cancer cells (the seed) and their host organ (the soil) collaborate to regulate the growth of tumor cells. Recent research has demonstrated that the metastatic progression of cancer is a multi-stage process that is more complicated than previously assumed [18]. Based on recent research, premetastatic niches can emerge and provide target organs with a metastatic orientation. The tumor cell is encouraged to colonize this particular milieu to spread to another target tissue [19, 20].

EMT is one of the important mechanisms inducing metastasis in the tumor microenvironment. Through EMT, cancer cells lose their epithelial properties and become more invasive, migratory, and resistant, which increases their ability to metastasize [21, 22]. Cells in the tumor microenvironment may also control metastasis through mechanisms that regulate EMT orientation. Furthermore, there is interaction between the immune system and the tumor microenvironment. Cancer cells can develop resistance against the tumor and immune system evasion by using EMT [23]. CSCs are part of the tumor microenvironment, which is constantly interacting dynamically with the immune system. Because of their exceptional capacity for self-renewal and differentiation, CSCs a more aggressive subgroup of tumor cells can also avoid immune cells, eluding the immune system and allowing the tumor to survive [24, 25].

Biochemical and metabolic components in the tumor microenvironment affect the immune cells. However, the most important cell groups affecting cell functions in the tumor microenvironment can be categorized into 2 groups: anti-tumor and pro-tumor. The anti-

tumor cell group represents tumor-fighting immune cells and consists of effector T cells, natural killer cells (NK), dendritic cells (DC), and M1-polarized macrophages. The pro-tumor group is the group of cells that promote tumor development and have suppressed immune responses. This cell group consists of Tregs, MDSCs, M2-polarized macrophages, N2-polarized neutrophils, natural killer T Type 2 cells (NKT2) cells, and ILC2 cells. These cell groups communicate with each other in the microenvironment through the cytokines they secrete into the TME [14, 26].

2.3. CYTOKINES

Cytokines are low molecular weight (~5-25 kDa) proteins that are either membrane-bound or secreted that function as intercellular signaling mediators to control the immune system's homeostasis [27]. They are generated in response to pathogens and tumor antigens by innate and adaptive immune cells [28]. They are important inflammatory agents in terms of quantity and diversity in the TME. Cytokines have subgroups such as interleukin (IL), interferon (IFN), tumor necrosis factor (TNF), and growth factor (GF) [29].

Cytokines interact via a group of shared and common receptors. Among the seven categories of cytokine receptors, Type I, and Type II cytokine receptors are the most researched in clinical settings because of their immediate reactivity [30]. The relationship between inflammation and tumor formation was first proposed by Rudolf Virchow in 1863 with the hypothesis that chronic inflammation causes tumor formation [31]. Research over the years has shown that chronic inflammation can be directed by a combination of cytokines, chemokines, inflammatory cells, and cancer cells to create a conducive environment for tumor growth [32]. Cytokines are molecular precursors that are directed to a target antigen of immune system cells and communicate with each other to form a response. While many forms of communication in the immune system occur directly through cell-cell interaction, the secretion of cytokines occurs in a versatile, efficient, and rapid manner. Cytokines are small proteins secreted by cells and have many functions such as regulating immunity, cell growth, hematopoiesis, and restoring damaged tissues [31, 32].

Cytokines are released over a period by nearly all cells, usually in response to stimulation. This release is short-lived due to the circulating half-lives of cytokines. Cytokines are detected by receptors on the plasma membrane of target cells that have a high affinity for

cytokines [31, 33]. The cytokine that binds to the receptor activates it, thereby triggering a series of intracellular signals. This stimulus reaching the cell nucleus affects gene transcription and influences important signals such as proliferation, differentiation, and cellular responses within the cell. Cytokines can also affect the cells (autocrine effect), nearby cells (paracrine effect), or distant cells (endocrine effect). Cytokines act on different cytokine receptors and elicit complex responses when they are released simultaneously. Synergy or antagonism between different cytokines is therefore a common feature that causes a high level of complexity. The ability of cytokine release to produce a wide range of effects by stimulating other cytokines is called a 'cytokine storm' [29, 32]. Cytokines are pleiotropic molecules that can have multiple effects, whose effects are determined by the target cell. Therefore, cytokines can have both pro- and anti-inflammatory effects. Cytokines that can support the immune system also act as immunosuppressants. Which side of the balance overcome in these two different behavioral choices can have a significant impact on cancer fate. An increasing number of studies have shown that systemic inflammation plays an important role in tumor development, progression, and clinical outcomes in a variety of human cancers, including non-small cell lung cancer, high-grade glioma, colorectal cancer, and renal cell carcinoma. Considering the relationship between inflammation, immunological response, and oncogenesis, the contribution of cytokines to this triad is important [32, 33].

Tumor development and growth are promoted in many cases by inflammatory cells that produce cytokines that stimulate the growth and survival of malignant cells. Inhibition of the pro-tumorigenic cytokine effect is important in providing therapeutic and preventive means [33, 34]. Considering this information, the effects of cytokines on tumors have not been determined. Cytokines released from the immune system and/or the tumor itself can be used as a signal to show a more aggressive profile (resistance to apoptosis, metastatic ability) by tumor cells. However, cytokines can also play an active role in the immune system’s defence mechanism against tumor cells. How these two opposing functions of cytokines alter the behavioral parameters of tumors is a question that needs to be explained in terms of tumor biology.

2.3.1. Role of the Cytokines on Immune Tumor Microenvironment

Cytokines are key mediators of cell signaling in the TME. The most comprehensive definition was made by Hanahan and Weinberg in 2011, which classified cancer survival capabilities and provided a detailed description of TME [33]. Inflammatory cells are extremely functional in the TME and there is an elevated accumulation of secreted inflammatory agents in the TME. They are released from many cell types, especially immune system cells. The cells that comprise the TME communicate through cytokines. This cell-cell communication drives tumor-determining processes in the microenvironment such as proliferation, invasion-metastasis, and angiogenesis [34–36]. Cytokines that play an active role in TME are secreted by inflammatory-immune cells. These cells are mainly tumor-associated macrophages (TAMs), tumor-associated neutrophils (TANs), myeloid-derived suppressor cells (MDSCs), DCs, NK cells, B cells, and T cells [34, 35].

The concentration of cytokines in the TME, their combined response, and diversity are of critical importance. Redundancy, the amount to which different cytokines have the same functional effects, is a crucial aspect of cytokine signaling. Because of this redundancy, altering one cytokine may compensate by altering another, which might make cytokine therapy more difficult [32, 37].

Soluble mediators are involved in paracrine signaling between the tumor microenvironment and the tumor. The most critical of these molecules are cytokines, chemokines, and growth factors. These molecules are critically effective in tumor progression [35]. These factors, which can be secreted both from tumor cells themselves and from other cellular components (such as cancer-associated fibroblasts, and endothelial cells) that make up the microenvironment, may mediate tumor growth and survival. In studies conducted for many years, it has been determined that many growth factors, cytokines, and extracellular matrix elements stimulate carcinogenesis by inducing EMT. TNF-α, TGF-ß, and interleukins are among the most frequently studied molecules in this field. When the relationship of this subject with chordoma is examined through the Brachyury connection; In an IL-8-related study, it was determined that increased Brachyury expression level increased the release of cytokines, chemokines, and angiogenic factors in the microenvironment. Again, because of the same study, increased Brachyury and increased expression of soluble elements indicate that EMT transmission in the cell is also increased [35, 37]. It can be thought that increased

Brachyury expression, which is one of the molecular markers of chordoma, may increase inflammation-mediated carcinogenesis by triggering an increase in cytokines in the cell. In another study, it was determined that cytokines secreted from macrophages, mast cells, neutrophils, and T cells, which are involved in immune defense in the tumor microenvironment, induce EMT transition by increasing the expression of EMT-related genes. This induction also supports the partial EMT state, which is a critical phase of cancer cells. It has been determined that some enzymes that support the increase in EMT cleave the connective tissue forming the ECM and inhibit E-cadherin synthesis, and thus tumor cells tend to mesenchymal phenotype. Because of these properties, cytokines are thought to be critical in determining the aggressiveness and fate of cancer [33, 37].

2.3.1.1. IL-6 Cytokine Signaling

The interleukin-6 (IL-6) is a robust, pleiotropic, inflammatory cytokine that belongs to the Type I cytokine receptor family. Numerous physiological processes of the immune system, such as inflammation and cell proliferation, lymphocyte developmental differentiation and cell survival, and the recovery of apoptotic signals, are actively regulated by the IL-6 signaling pathway [38, 39]. IL-6 is produced by various immune cells such as macrophages and T cells in response to infection, injury, or inflammation. IL-6 binds to IL-6 receptor (IL-6R), on the surface of target cells. There are two forms of IL-6 receptors: membrane-bound IL-6R (mIL-6R) and soluble IL-6R (sIL-6R) [40].

IL-6 binds to the receptor IL-6 and forms an IL-6/IL-6R complex. IL-6R consists of the IL-6R subunit (also known as CD126) and the gp130 subunit (also known as CD130; encoded by IL6ST). Structure-function studies suggest that a functioning IL-6 receptor requires the formation of an IL-6/IL-6R/gp130 complex clustered into a dimer construct [41, 42]. Although gp130 is characterized as the signal subunit of the IL-6 receptor, signaling via gp130 is also important for growth, hematopoiesis, cell survival, and growth. Therefore, gp130 is also present in immune system cells and other cells that are not present in the immune system and hence the deletion of gp130 in mice in the literature has resulted in embryonic death. Once the IL-6 receptor complex is activated, many downstream pathways are activated to mediate the different effects of IL-6. The binding of the IL-6 ligand to the heterodimer complex formed by the IL-6 receptor protein and the gp130 protein enables phosphorylation by activating the kinases of the JAK (Janus Kinase) family. The phosphorylated JAK proteins enable the phosphorylation of STAT1, STAT3 proteins. The

gp130 labelling of JAK-STAT is strictly controlled and PIAS (active STAT protein inhibitor) inhibitors of active STATs suppress the SOCS cytokine signal. In addition, members of the CIS family (including cytokine-inducible SH2-domain) limit the activation of IL-6 cytokine receptor inhibitors. In this receptor complex, the role of the IL-6 molecule in homeostasis and the fact that the gp130 protein has important functions in many cells supports the idea that the molecule that needs to be focused on is IL-6R [41–44].

IL-6 uses two different ways to perform its biological function. Accordingly, the "classical" IL-6 receptor signaling refers to activities performed by the membrane-bound IL-6R subunit and relates only to cells expressing both receptor subunits (IL-6R and gp130). In addition, “trans” IL-6 receptor signaling refers to a process in which the soluble IL-6R (sIL-6R) form binds to the secreted IL-6 to form a complex that enhances the circulating half-life and bioavailability of IL-6. Classical IL-6 receptor signaling, as well as central homeostatic processes also control immunological responses such as glucose metabolism, acute phase response, hematopoiesis, and regulation of the neuroendocrine system. Soluble IL-6R is released by monocytes and activated T cells and IL-6 trans-signaling is important for allergy, infection, inflammatory arthritis, neuro-inflammation, and infection-related cancers [42–44].

Considering severe inflammatory diseases are caused by elevated IL-6 production, both transcriptionally and post-transcriptionally, IL-6 expression is strictly controlled. The activation of the IL-6 promoter region is triggered by inflammatory cytokine receptor signaling, which is one of these regulatory mechanisms that engage cis-regulatory elements. The stability of IL-6 mRNA is controlled by a variety of RNA-binding proteins that bind to the 3'-UTRs, such as Arid5a (AT-rich interactive domain-containing 5a). Arid5a binds to IL-6 mRNA and allows it to maintain its stabilization. Conversely, degradation of IL-6 mRNA is processed to suppress excess IL6 production in the environment. Regnase-1 is a protein with endonuclease activity that binds to the stem-loop motif in the 3’-UTR regions of IL-6 mRNA. Arid5a binds directly to IL-6 mRNA and stabilizes it by neutralizing the activity of Regnase-1 in macrophages [44–47].

Several types of cancer have been associated with increased levels of IL-6 and have been found to contribute to cancer progression [45–47]. The development and survival of cancer cells can be enhanced by IL-6. It has the ability to trigger signaling pathways that promote both decreased apoptosis and increased cell proliferation. In another way, IL-6 is a

proinflammatory cytokine. A well-established risk factor for cancer is chronic inflammation, and IL-6 plays a crucial role in the inflammatory response [34]. It could trigger the release of other inflammatory mediators that can create a microenvironment conducive to cancer development. The functions of IL-6 signaling most associated with cancer are related to its proliferation and its role in the microenvironment. Studies has associated IL-6 to chemotherapy resistance, metastasis, and angiogenesis [46, 48].

Early-stage and translational findings demonstrate that IL-6 has an important role in various malignant tumors and provide a biological rationale for targeted therapeutic research. More evidence supporting the pathogenic role of IL-6 in cancer has come from the effective application of corticosteroids, nonsteroidal anti-inflammatory drugs, and estrogen-derived drugs which inhibit IL-6 signaling in the treatment of various diseases. The emphasis of IL-6 and IL-6R, however, is essential for direct targeted therapy. Three commonly used and clinically approved IL-6 antagonists are siltuximab (an anti-IL-6 mAb), tocilizumab and sarilumab (anti-IL-6R mAb). The literature involve clinical trials for cancers such as multiple myeloma, prostate cancer, and ovarian cancer that have a promising preclinical rationale supporting IL-6 signaling inhibition [37, 49] (Table 2.1).

IL-6R mediates the signaling of IL-6 and this cascade can affect various aspects of cancer biology. In recent years, the development of therapies targeting IL-6R has gained clinical relevance. Clinical practice uses monoclonal antibodies that block IL-6R, like tocilizumab, to treat diseases like COVID-19 and rheumatoid arthritis [50–52]. Researchers are exploring their potential in cancer treatment, both alone and in combination with other therapies. Clinical research also focuses on the relationship between IL-6R and the immune system. Immunotherapies such as immune checkpoint inhibitors may be more effective when IL-6R is blocked. This may also impact the immune response to the tumor microenvironment. Several clinical trials are in progress to evaluate the efficacy and safety of targeting IL-6R in various types of cancer.

Table 2.1. Research on IL-6R and cancer is included in the list of clinical trials.

Study Title	NCT Number	Status	Conditions
Feasibility of the Combination of Chemotherapy (Carbo/Caelyx or	NCT01637532	Completed	Recurrent Ovarian Cancer

Carbo/Doxorubicin) With Tocilizumab (mAb IL-6R) and Peg-Intron in Patients With Recurrent Ovarian Cancer			
A Safety, Efficacy and Pharmacokinetic Study of Siltuximab (CNTO 328) in Participants With Solid Tumors	NCT00841191	Completed	Ovarian/Pancreatic/Colorectal/2more Neoplasms
Trastuzumab and Pertuzumab in Combination With Tocilizumab in Subjects With Metastatic HER2 Positive Breast Cancer Resistant to Trastuzumab	NCT03135171	Completed	Breast Cancer
Phase I Study of the Combination of Afatinib and Ruxolitinib in Patients With Treatment-refractory Non-Small Cell Lung Cancer (NSCLC)	NCT02145637	Completed	NSCLC
Simvastatin With Topotecan and Cyclophosphamide in Relapsed and/or Refractory Pediatric Solid and CNS Tumors	NCT02390843	Completed	Retinoblastoma/Clear/Renal Cell Sarcoma/9more
A Phase I, 2-part (Part 1 Being a Single Dose Escalation and Part 2, a Parallel Group) Study of Toll-like Receptor (TLR4) Agonist (GSK1795091) in Healthy Subjects	NCT02798978	Completed	Cancer/Neoplasms
Lenalidomide and Temsirolimus in Treating Patients With Previously Treated Multiple Myeloma	NCT00398515	Completed	Refractory/Stage II/Stage III/Multiple Myeloma
A Safety and Efficacy Study of CNTO 328 in Patients With B-Cell Non-Hodgkin's Lymphoma, Multiple Myeloma, or Castleman's Disease	NCT00412321	Completed	Non-Hodgkin Lymphoma/Multiple Myeloma/Giant Lymph Node Hyperplasia
Safety and Efficacy of KTE-C19 in Combination With Atezolizumab in Adults With Refractory Diffuse Large B-Cell Lymphoma (DLBCL)	NCT02926833	Completed	Refractory DLBCL
Study Evaluating the Safety and Efficacy of KTE-C19 in Adult Participants With Refractory Aggressive Non-Hodgkin Lymphoma	NCT02348216	Completed	Refractory DLBCL/Relapsed DLBCL/Transformed Follicular Lymphoma (TFL)/2more

Clinical trials listed in Table 2.1 include IL-6R-related cancer studies. These studies are completed trials. In addition, there are 6 other trials in the recruitment phase. These studies

aim to determine the potential benefits of IL-6R-targeted therapies and their role in improving patient outcomes.

The investigation of IL-6 signaling in chordomas

Research regarding the effect of IL-6 signaling in chordoma are limited in the literature. According to Wang et al., the effect of FTY720, an immunosuppressive agent, on chordomas was examined and the findings showed that this molecule reduced proliferation and EMT in chordomas through IL-6/STAT3 inhibition [53]. However, this article has been retracted. Apart from this, there are no articles directly investigating chordoma and IL-6 signaling. There are some studies on chordoma microenvironment and indirect associations with IL-6 signaling via other molecules [55]. One of them revealed that LIF, a cytokine in the IL-6 family, LIF is involved in controlling the proliferation of cancer stem cells, including those found frequently in chordoma. In chordoma cell lines, the expression of LIF boosted cell motility and invasiveness [54].

3. METHODOLOGY

In this section, experimental studies were conducted to determine the targeting of the IL-6 receptor and its functional/transcriptomic effects in the chordoma cell lines.

3.1. CHORDOMA CELL CULTURE MAINTENANCE

In this research, chordoma cell lines were cultured *in vitro* in a 4:1 ratio of Iscove's Modified Dulbecco's Medium (IMDM): Roswell Park Memorial Institute (RPMI) 1640 Medium containing 10% Fetal Bovine Serum (FBS), 1% Penicillin-Streptomycin (PS). The culture flasks used in chordoma culture were covered with 0.1% gelatine. In the prepared gelatine-coated cell flasks, $4x10^5$ chordoma cells were added in 12ml medium and incubated at 5% CO^2, 1 atm pressure, and 37ºC temperature. The medium was changed every other day until the cell density reached 80% of the flask. After reaching the appropriate density, 0.25% trypsin-EDTA was used to passage the cells. The experiments were carried out using two chordoma cell lines: primarily based and sacrum located JHC7, recurrent based and sacrum located MUG-Chor1.

3.2. TARGETING THE IL-6R GENE FOR SILENCING

The interleukin-6 receptor gene was targeted to determine the effects of the IL-6 cytokine pathway on chordoma cell lines. CRISPR/Cas9 knock-out and shRNA lentiviral systems were used to knock-out/down IL-6R gene expression.

3.2.1. IL-6R Gene Silencing via CRISPR/Cas9 Knock-out (KO) System

The CRISPR-Cas9 (Clustered Regularly Interspaced Short Palindromic Repeats/Cas9) system, which is a natural defense mechanism in prokaryotes, has been redesigned in current technology and used as a gene editing technology. The system basically consists of two components: Cas9 (CRISPR-associated protein 9), an endonuclease that allows cutting the target DNA, and a guide RNA that matches the target gene [56]. The transfer of gRNA and Cas9 protein into the target cell is accomplished through transfection, viral vectors, or other delivery methods. Cas9 protein is directed to the DNA location in the target gene via gRNA. The endonuclease activity of Cas9 causes a double-strand break (DSB) at a specific DNA

location. This break triggers DNA repair mechanisms in the cell. There are two mechanisms the cell uses to repair double-stranded DNA damage: non-homologous end joining (NHEJ) and homology-directed repair (HDR). In systems designed to knock-out the target gene, the cell's NHEJ repair mechanism is triggered. It thus introduces mutations that disrupt the function of the target gene to effectively eliminate its expression [56, 57]. This study aimed to silence IL-6R gene expression in MUG-Chor1 and JHC7 chordoma cell lines via the CRISPR/Cas9 system. For this purpose:

Commercially available CRISPR/Cas9 IL-6R KO plasmid (Santacruz, Cat. No. sc-400582-KO-2) and HDR plasmid (Santacruz, Cat. No. sc-400582-HDR-2) were used in this study (Figure 3.1). The combination of these two plasmids was designed to provide cells with the option of selection. The transduction-ready plasmids were transduced into chordoma cells using FuGENE HD (Promega, Cat no: E2311). After 48 hours, cells with inhibited IL-6R gene expression were selected by puromycin antibiotic treatment.

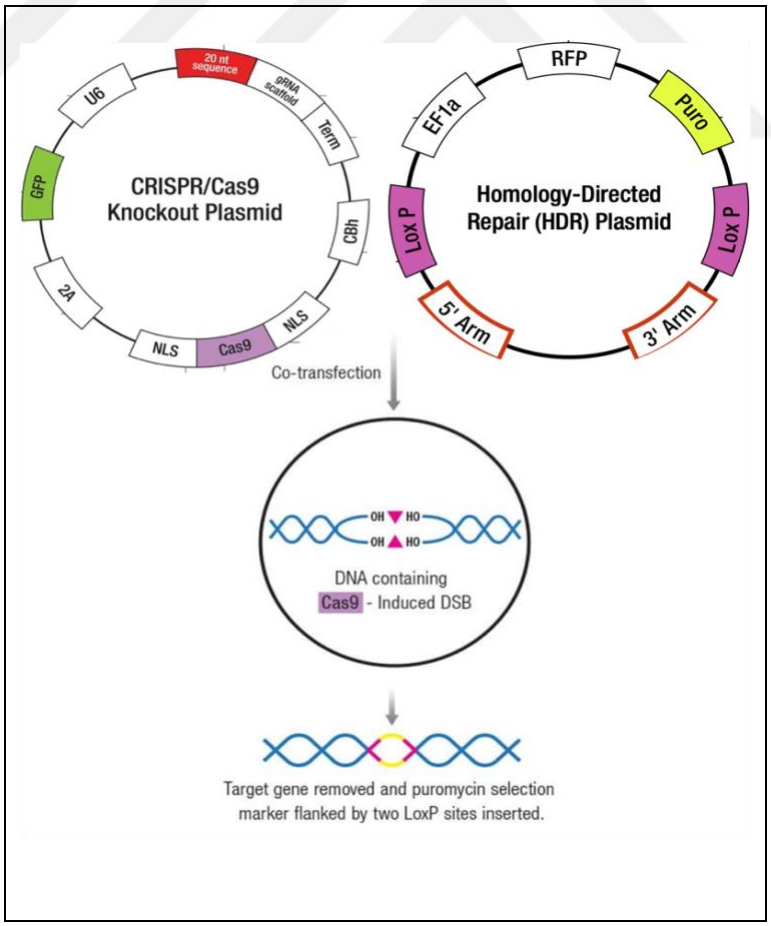

Figure 3.1. Mechanism of action of CRISPR/Cas9 KO and HDR plasmids co-transfection

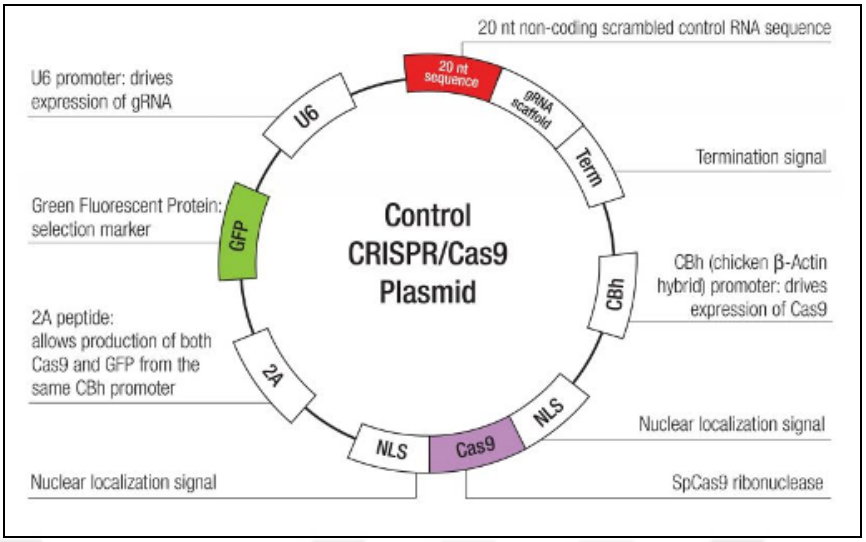

Figure 3.2. Control CRISPR/Cas9 plasmid map

Cells transduced with "Control CRISPR/Cas9 Plasmid (sc-418922)" were used as the control group of the study. Cells transduced with "Control CRISPR/Cas9 Plasmid (sc-418922)" were used as the control group of the study (Figure 3.2). The control group was subjected to the same procedures as the experimental group.

Electroporation is a physical method of transfection that makes the cell membrane permeable by applying an electric pulse and moving molecules into the cell with an electric field [58, 59]. Electroporation could be unsuccessful for a variety of reasons, including the size of the DNA fragments to be transfected as well as the level of toxicity [60]. A unique combination of cell type-specific solutions and customized electrical parameters, known as Nucleofection® Technology, enables the transfer of a molecule directly into the nucleus of a cell. Because it is not dependent on cell division, it can effectively transfect even quiescent primary cells (such as T cells or neurons) and speed up expression [61–63].

The manufacturer's recommended protocol was carried out. Two different solutions were used to apply the Control plasmid and the IL6R KO plasmid to the JHC7 and MUG-Chor1 cell lines. PmaxGFP Plasmid was used as a control. Flow cytometry was used to evaluate the results.

3.2.1.1. DNA Laddering Assay

Apoptotic DNA fragmentation is an essential stage of apoptosis. The process of apoptosis involves the cleavage of nuclear DNA into internucleosomal fragments, which is followed by the activation of endogenous endonucleases. One of the golden standards used for apoptosis detection is the DNA laddering assay, which determines DNA fragmentation [64–67]. In this study, DNA of the cells was collected from the cell culture dish and isolated by DTAB/CTAB method. DNA samples were run on a 2% agarose gel using TAE Buffer at 40V current for approximately 2 hours/+4°C. Cisplatin-treated cell DNA was used as a positive control.

3.2.2. Lentiviral shRNA-mediated IL-6R Gene Silencing

The shRNA (short hairpin RNA) system is used to down-regulate or knock-down the expression of a targeted gene in the cell. This system involves the use of short hairpin RNA molecules, synthetic RNA sequences that can induce RNA interference (RNAi) [68]. shRNA molecules are designed to be complementary to the mRNA of the target gene. These molecules contain a hairpin loop structure and are approximately 19-29 base pairs. By cloning shRNA sequences into expression vectors that may be inserted into target cells, the target cell produces shRNA molecules. Vectors introduced into the target cell via transfection enable the cell to produce shRNA molecules. Cellular mechanisms of the target cell convert shRNA molecules into small interfering RNAs (siRNAs). These siRNAs then direct the RNA-induced silencing complex (RISC) to the target mRNA. The RISC complex binds to the target mRNA, leading to its degradation or translational repression. This effectively reduces the expression of the target gene [68, 69].

3.2.2.1. Amplification of IL6R-shRNA plasmids

The pGFP-C-shLenti vectors (IL-6R Human shRNA Plasmid Kit (Origene, cat no: TL312161) were used in the study. The kit contains four shRNAs targeting IL-6R and one transfection control.

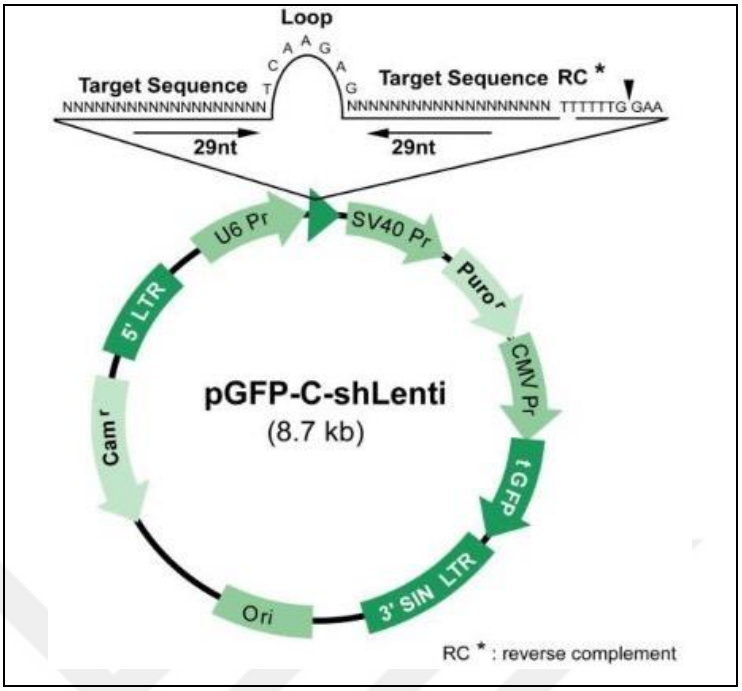

Figure 3.3. IL-6R Human shRNA Plasmid map

Table 3.1. Sequences of shRNAs and their nomenclature in the present study.

Name	Cat No:	Sequence
Control SH	#TL312161	GCACTACCAGAGCTAACTCAGATAGTACT
SH1	#TL312161A	ACAAAGGCTGTGCTCTTGGTGAGGAAGTT
SH2	#TL312161B	TAGAGCCGAAGACAATGCCACTGTTCAC
SH3	#TL312161C	TCTACATAGTGTCCATGTGCGTCGCCAGT
SH4	#TL312161D	CGAAGACTTCCAGGAGCCGTGCCAGTATT

Bacterial transformation of plasmids was achieved by using the *Escherichia coli* (E. coli) bacterial-DH5α strain, which was competent by Inoue protocol. For bacterial selection, transformed bacteria cells were inoculated in LB agar culture dishes containing chloramphenicol (34 ug/ml) and incubated at 37ºC overnight. The next day, a single cell colony was selected from the proliferating bacterial colonies and inoculated into LB Broth containing chloramphenicol. The single-cell colony was incubated overnight at 37ºC in a shaker rotor incubator. The next day, the proliferating single bacterial cell colony was centrifuged at 2500rpm for 20 min.

DNA isolation of shRNA plasmids from the obtained bacterial cells was performed with GeneJET Plasmid Miniprep Kit (Thermo, Cat no: K0502).

Restriction digestion was performed with FastDigest kit (Thermo, Cat. No: B72) and enzymes. Samples were prepared according to the protocol recommended by the company. The enzymes selected for digestion were determined using the plasmid map and SnapGene tool. According to the inactivation conditions of EcoRI and XbaI enzymes, the mixture was incubated at 80ºC for 20 min. The samples were then run on a 1% agarose gel and visualized under UV light.

3.2.2.2. Lentiviral Transfection

Transfection was performed using FuGENE HD (Promega, Cat no: E2311) according to the protocol recommended by the company. Lentiviral vectors were transfected into HEK293FT cells using VSV-G (Addgene) and dVPR (Addgene) plasmids. The 2nd generation plasmids lenti-shRNA: dVPR:VSV- G (ratio: 10: 10: 1) was used for virus generation. The medium in the cells was changed 24h after transfection and virus supernatants of 48th and 72nd hours were collected. The collected virus supernatants were separated from HEK293FT cells by passing through a 0.45µm sterile filter.

3.2.2.3. Transduction of chordoma cell lines

One day before transduction, chordoma cells were seeded in 6-well cell growth dishes. Chordoma cells at 60% density on the day of the experiment were incubated with OPTI-MEM medium (FBS and antibiotic-free medium) 2 hours before transduction. At the end of the time, Opti-MEM was removed from the cells and replaced with 2ml of virus supernatant (containing polybrene at a concentration of 4 µg/ml). The culture dish was centrifuged at 1200 rpm for 2 hours (at 27ºC). At the end of centrifugation, the virus supernatant on the chordoma cells was replaced with a fresh medium and incubated overnight. Fourty-eight hours after transduction, methods for establishing stable cell line steps were performed.

3.2.2.4. Generating stable chordoma cell lines

After the transduction of chordoma cell lines with IL-6R shRNA plasmids, the cell lines were subjected to a series of selections to maintain stable silencing efficiency.

IL-6R shRNA plasmids contain a eukaryotic antibiotic selection gene that is selective for puromycin. Therefore, puromycin selection is performed in transduced cells. Prior to selection, determining the optimal dose of puromycin for each cell line is crucial. The puromycin killing curve is generated by subjecting the chordoma cells at different dose ranges over 15 days and their viability was determined by MTS at the end of 15 days. The minimum dose that killed 100% of the cells was selected as the puromycin dose to be used.

48h after transduction, cells were subjected to puromycin selection for 1 week. In transduced cell lines, cells that successfully integrate the plasmid into the genome are expected to resist puromycin and survive.

After puromycin selection, a second selection was made by fluorescent sorting. In case of successful transduction, the GFP selection gene in the plasmid map is expected to be integrated into the cell genome and the cells are expected to fluorescence GFP. JHC7 and MUG-Chor1 cells were stained with DAPI and GFP (+) fluorescent cell populations were selected by flow cytometry (BD FACSAria™ III). The selected green population was separated from the main population by FACS. This process was repeated twice for a pure GFP (+) population. These cells can be stably identified as having silenced the IL6R gene.

3.2.2.5. Evaluation of IL-6R gene silencing

The silencing efficiencies of IL-6R were checked by qRT-PCR at the mRNA level and Western blot at the protein level.

cDNA synthesis and Quantitative Real-Time Polymerase Chain Reaction

Changes in IL-6R gene expression were analyzed by quantitative real-time polymerase chain reaction (qRT-PCR) to control silencing. To convert the isolated RNA samples into complementary DNA (cDNA) sequences, cDNA synthesis was performed with the High-Capacity cDNA Reverse Transcription kit (Applied Biosystems®, Catalog. No: 4368814) by the company protocol.

Gene expression analysis was performed with the StepOne™ device using TaqMan Universal PCR Master Mix (Thermofisher, Catalog No: 4304437) according to the manufacturer's instructions. The probes used in real-time polymerase chain reactions were purchased commercially, and YWHAZ was preferred as a housekeeping reference gene to ensure normalization between the experimental groups. Statistical analyses were performed by two-way ANOVA test and calculations and graphs were prepared with GraphPad Prism version 9.5.0 software.

Total protein isolation and Western blot assay

Western blotting was performed with IL-6Rα-specific antibody (IL-6Rα/CD126-Rabbit mAb #18935, CST) via Mini-PROTEAN® Tetra Cell, Mini Trans-Blot® Module, and

PowerPac™ Basic Power Supply (Bio-Rad, 1658033) in the laboratory. GAPDH-specific antibody (D16H11 XP® Rabbit mAb #5174, CST) was used as an internal control.

Total protein isolation of cell groups was carried out using “RIPA (CST, Cat No: 9806)” with the addition of “Phosphatase & Protease inhibitor solution (Thermo Scientific, Cat No: 78440)”. Protein concentration was determined using “Pierce BCA Protein Assay Kit (Thermo Scientific, Cat No: 23225)”. Proteins were separated by 12% SDS-PAGE (TGX™ FastCast™ Acrylamide Kit, Bio-Rad, Cat no: 1610175) electrophoresis and transferred to PVDF membrane (Polyvinyl fluoride 45mm, Thermo Scientific, cat no: 88518). Then, the membranes were blocked in 2.5% BSA (Bovine Serum Albumin, Sigma-Aldrich, Cat no: A9647) solution. Antigen–antibody complexes were formed with Horseradish Peroxidase (HRP)-carrying secondary antibody (Invitrogen Life Technology) and the resulting luminescence was obtained using chemiluminescence irradiation (Clarity Western ECL Substrate kit, BIO-RAD, Cat no: 1705061). After imaging, the analysis of the protein bands was made using the "ImageJ (Image Processing and Analysis in Java)" program.

3.2.2.6. Evaluation of IL-6R silencing via Tocilizumab

The IL-6R humanized monoclonal antibody, FDA-approved immunosuppressive drug, Tocilizumab (TCZ, Actemra) was used as an alternative to IL-6R silencing in chordomas. For one week, TCZ was administered to JHC7 and Mug-Chor1 cells. A range of TCZ doses utilized in the literature for *in vitro* cell culture was determined for the provided dose (10-20-30 μg/ml) [70–72]. The stable cells generated with the SH3 plasmid were used to establish the comparison group, IL-6R-shRNA, which was determined to have the highest silencing effectiveness.

3.3. THE WHOLE TRANSCRIPTOME ANALYSIS

The Clariom D total transcriptome array is a comprehensive microarray system that enables the detection of more than 540,000 codings and non-coding (long non-coding RNAs, circular RNAs) transcriptomes as well as their alternative splicing events. Gene expression profiles of JHC7 and MUG-Chor1 cells in IL-6R silenced and control cell groups were obtained using Clariom D Total Transcriptome Microarray kit (Affymetrix, Cat no: 902923) and GeneChip-3000 microarray system. Experiments were performed repeatedly for each group.

Microarray experiments performed according to the manufacturer's instructions (GeneChip™ WT PLUS Reagent Kit user guide) consisted of amplification, purification, fragmentation and labeling, hybridization, wash & stain, and scan. TRIzol isolated total RNA by the manufacturer's instructions (Thermo Fisher Scientific, Waltham, 15596026). To obtain single-stranded cDNA, 250 ng of total RNA samples were poly-A-tailed and synthesis processes were followed. In the following step, the single-stranded cDNA was fragmented and labeled. The GeneChip® Hybridization Oven 645 was used to hybridize labeled samples on GeneChip arrays for 16 hours at 45°C and 60 rpm. Labeled samples were hybridized on GeneChip arrays at 45ºC and 60 rpm for 18 h via GeneChip® Hybridization Oven 645. The arrays were washed, stained, and scanned using the GeneChip® Fluidics Station450 and GeneChip® Scanner3000 7G System. Affymetrix® Transcriptome Analysis Console (TAC, version 4.0) was used for analyzing differentially expressed RNAs within the study groups. The workflow diagram of the protocol followed is presented in Figure 3.4.

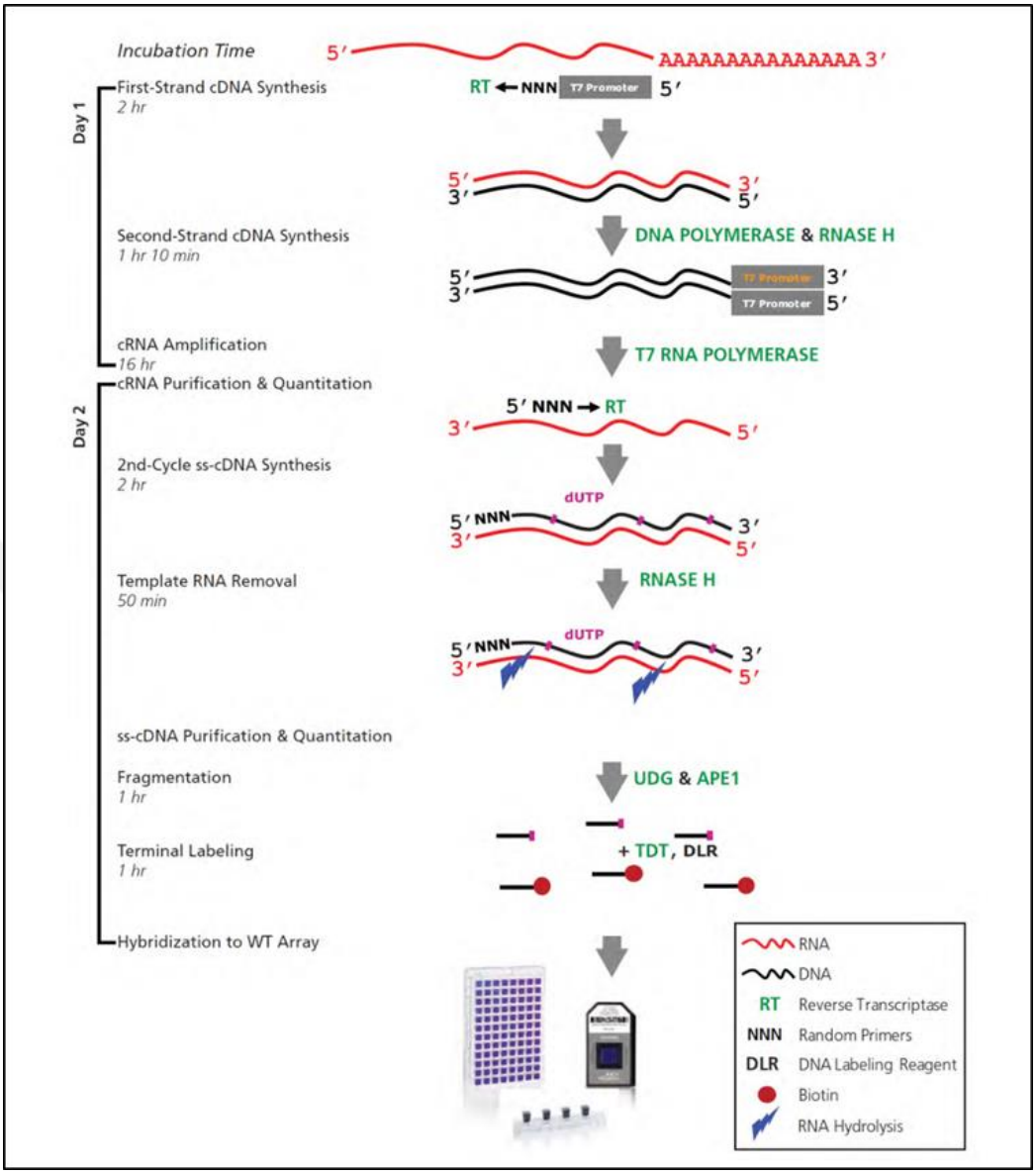

Figure 3.4. Flowchart of microarray experiment

The Transcriptome Analysis Console (TAC) program provided by Affymetrix was used to process and interpret the raw data. The robust Multichip Average (RMA) method was used for background correction, normalization, and summarization of raw microarray data in CEL format. The raw data to be analyzed were converted to CHP format. GRCh38 (*Homo sapiens*) reference was used for annotation of transcription events.

In the evaluation of the altered transcriptome in IL-6R silenced cells compared to control groups, significant alterations at the gene and exon levels are those with absolute fold changes more than 2 and p values less than 0.05. TAC Software/WikiPathways and The

Database for Annotation Visualization and Integrative Discovery (DAVID) databases were used for functional enrichment analysis of genes with significantly altered expression.

3.4. DETERMINATION OF FUNCTIONAL ALTERATIONS

In this section, a series of experiments were performed to determine the functional effects of IL-6R gene silencing in chordomas.

3.4.1. Migration and Invasion Assays

Boyden chamber assay was performed to evaluate the migration and invasion capacity of IL6R gene silenced cells. For this experiment, transwell inserts with a pore width of 0.8 uM were used, which can be placed in 24-well cell culture plates. The experiment is based on the principle of determining the capacity of cells cultured in serum-free medium to "migrate" to serum-containing medium by chemotaxis. The same experimental setup is used to evaluate the "invasion" capacity of the cells when transwell inserts with a 250 ug/mL matrigel-coated substrate are used. The stages of the experiment are as follows:

For migration assay, cells were made into single-cell suspension with trypsin, washed with DPBS, and serum medium, and trypsin was removed. Cells were counted by thawing in serum-free medium and added into transwell inserts as 40,000 viable cells/200µL medium. Inserts with cells were placed in 24-well cell culture plates supplemented with 1300 µL of chordoma medium containing 20% FBS. Cells were incubated for 48 hours under culture conditions (37ºC, 5% CO^2).

The cells were fixed and stained at the end of the migration procedure. For this purpose, the staining protocol with Crystal Violet dye was applied:
The inserts are washed 2 times with PBS after the medium is poured out. Formaldehyde (3.7%) is added to the inserts and allowed to fix at room temperature for 4 minutes. The inserts are washed 2 times with PBS to remove the formaldehyde. Methanol (100%) added to the insert and fixed the cells on the surface of the insert for 20 minutes at room temperature. Inserts were washed twice with PBS to remove methanol.

For staining of the cells, 0.1% Crystal Violet solution was added into a 500µL insert, 500µL was added to the well below and the cells were kept in the dark for 2 minutes at room temperature. Inserts were washed twice with PBS to remove some of the dye from the inserts. The inserts were left in a dark place for a few hours to dry and then the cells are counted under a microscope.

3.4.2. Tumor-sphere Formation Assay

The tumor-sphere form is the name given to the solid spherical form formed by the division and proliferation of cancer stem cells [73, 74]. It is formed by culturing heterogeneous cancer cell populations in a serum-free medium without an adherent surface. In this study, 50×10^3 cells were seeded in serum-free culture medium in low-attachment 24 well-plate culture dishes. Culture was continued until tumor spheres were formed (1-2 weeks). During this period, 1mL of the medium was withdrawn from the culture dish every 2 days without any contact with the spheres and fresh sphere medium was added.

As sphere medium: 10 µl EGF recombinant human protein (20ng/ml) (Thermofisher, Catalog No: PHG0311), 10 µl BFGF recombinant human protein (20ng/ml) (Thermofisher, Catalog No: 13256029), 1000 µl B27 supplement (50X) (Thermofisher, Catalog No: 17504044) and 500 µl N2 supplement (100X) (Thermofisher, Catalog No: 17502001) dissolved in 50 ml FBS-free culture medium.

3.4.3. Scratch Assay

The effect of IL6R silencing on the capacity of cells to migrate in two dimensions under *in vitro* conditions was examined. At the beginning of this experiment, the cells were allowed to reach 100% density in the culture dish. Then, a scratch of equal width and length was created in each well using a sterile pipette tip. The wells were observed and images were recorded at 0, 48, and 96 hours until the scratch/gap was closed. Images were analyzed using Image-J software. The results were evaluated for each cell line by comparing the control group and IL-6R gene-silenced cells.

3.4.4. Evaluation of Cancer Stem Cell Expressions and Epithelial to Mesenchymal Transition

In chordoma cell lines, IL-6R silencing was also assessed in terms of Cancer Stem Cell (CSC) and Epithelial to Mesenchymal Transition (EMT). An investigation was conducted to examine to measure the levels of CSC/EMT-related genes *NANOG, OCT4, SOX2, CDH2 (N-CAD),* and *VIM*. The probes used in real-time polymerase chain reactions were purchased commercially, and *YWHAZ* was preferred as a housekeeping reference gene to ensure normalization between the experimental groups. Statistical analyses were performed by two-way ANOVA test and calculations and graphs were prepared with GraphPad Prism software.

3.5. STATISTICAL ANALYSIS

Quantitative Real-time PCR data were statistically evaluated for relative gene expression changes (2^-ΔΔCt) using an unpaired t-test based on the -ΔΔCt values of the relevant genes. Statistical significance was defined as p values less than 0.05. GraphPadPrism version 9.5.0 (San Diego, California, USA) was used to perform statistical data analysis on the qRT-PCR and western blot data, migration, invasion, tumor-sphere, and scratch assays.

4. RESULTS

A series of experiments were performed to determine the efficacy of IL-6 signaling in chordoma cell lines. The main molecule focused on for this purpose is the IL-6R, the receptor for the IL-6 cytokine. By silencing the IL-6R gene in chordomas, the effectiveness of signaling was examined by different experiments.

4.1. TARGETING THE IL-6R GENE FOR SILENCING

4.1.1. CRISPR/Cas9 KO & HDR System

Chordoma cells were transduced utilizing the FuGENE HD agent and the IL-6R CRISPR/Cas9 KO & HDR plasmid by the manufacturer's instructions. The control CRISPR/Cas9 plasmid was used as the control plasmid. The IL-6R KO group's chordoma cells were not viable in comparison to the control group. Additional experiments were carried out with other agent: DNA ratios to minimize the cytotoxic effect of the used substance, but no viable cells were observed.

In another gene transfer method, electroporation via nucleofactor, experiments were performed using different voltage and buffer options. As a result of previous optimization attempts, DS150 and CM137 solutions were used (optimized electrical parameters and cell type-specific solutions) (Table 4.1). Nucleofection was performed for both the IL-6R KO Plasmid and the Control Plasmid.

Table 4.1. Nucleofactor protocols were used in the study according to cells.

Well	Cell	Plasmid	Protocol	Kit
A1	JHC7	IL6R KO	DS 150	SF
A2	JHC7	IL6R KO	CM 137	SF
B1	JHC7	Control P	DS 150	SF
B2	JHC7	Control P	CM 137	SF
C1	MugChor1	IL6R KO	DS 150	SF
C2	MugChor1	IL6R KO	CM 137	SF
D1	MugChor1	Control P	DS 150	SF
D2	MugChor1	Control P	CM 137	SF
GFP	MugChor1	pmaxGFP	DS 150	SF

However, while successful electroporation was achieved in the pmaxGFP plasmid used as a control group, viable chordoma cells could not be obtained in the IL-6R CRISPR/Cas9 KO & HDR plasmid group. In the control groups, it was confirmed that the methods worked properly (Figure 4.1). Both gene transfer methods' findings suggest that knocking out the IL-6R gene alters vital cell activities and terminates cell viability. The literature shows that in a similar manner, *in vivo* mouse death occurs when the gp130 molecule, which is implicated in IL-6 signaling, is knocked out in mice [75]. The IL-6R gene might be regulated by a similar process. The same investigations were carried out with HEK293FT cells, which are known to be easily transfected, to gain insight into this. The results showed that HEK293FT cells had colonies that were still alive, despite their relatively low viability efficiency. It was investigated whether the IL-6R gene knock-out caused these few cells to undergo apoptosis, like chordomas.

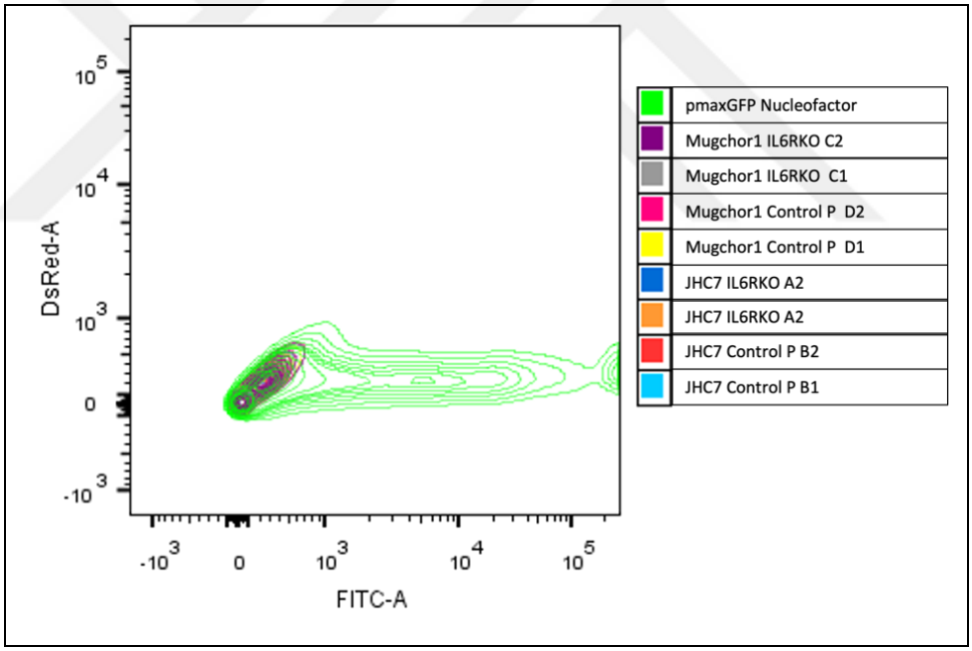

Figure 4.1. Flow cytometry data was obtained by the knockout experiment with Nucleofector.

4.1.1.1. Determination of Apoptosis via DNA Laddering Assay

DNA laddering assay was used for apoptosis detection in IL-6R knock-out HEK293FT cells. This assay is preferred because it provides an apoptosis detection that can be used with lysate from small quantities of living cells [65].

Cisplatin chemotherapeutic agent was administered to HEK293FT cells as a positive control (PC) to induce apoptosis. The agarose gel image of the experimental groups transfected with the control KO plasmid and HEK293FT IL-6R KO plasmid was determined. (Figure 4.2.)

DNA fragmentation structure revealed an orientation toward apoptosis in both the IL-6R KO HEK293FT cells and the positive control group [76]. There was no evidence of a fragmented band structure, indicating an absence of apoptotic orientation, in the negative control group.

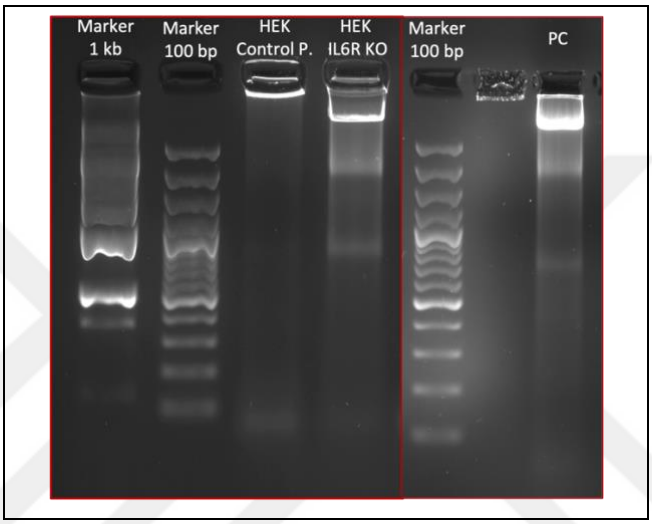

Figure 4.2. DNA fragmentation assay gel image. PC; Positive control, HEK293FT cells apoptosis induced by cisplatin treatment.

4.1.2. Lentiviral shRNA System

IL-6R shRNA plasmids purchased commercially from Origene contain 4 different guide RNA (gRNA) constructs and scramble (control) shRNA. Before starting the experiments, the plasmids were amplified in bacterial systems. After transformation and plasmid DNA isolation, restriction enzyme digestion was performed to select the correct plasmid.

4.1.2.1. Amplification and Restriction Digestion of shIL6R Plasmids

DNA isolation was performed from the plasmids amplified in bacterial cells as a result of transformation. Colony validation was performed for each shRNA construct. Restriction-cutting enzymes, EcoRI & XbaI, in the plasmid map were used for the confirmation of the amplified IL-6R shRNA plasmid. After the enzyme cutting, agarose gel electrophoresis was performed. Thus, depending on the size of the DNA fragments expected after cutting, it was proved that the replication was carried out with the correct colony selection.

After restriction digestion of the plasmid, the SnapGene tool was used to determine the band lengths expected to be observed in the gel. As shown in Figure 4.3a, when dual-cutting with EcoRI and XbaI enzymes, two bands of 1653 bp (fragment between the two enzymes selected in blue) and 7038 bp (remaining fragment of the plasmid) should be observed.

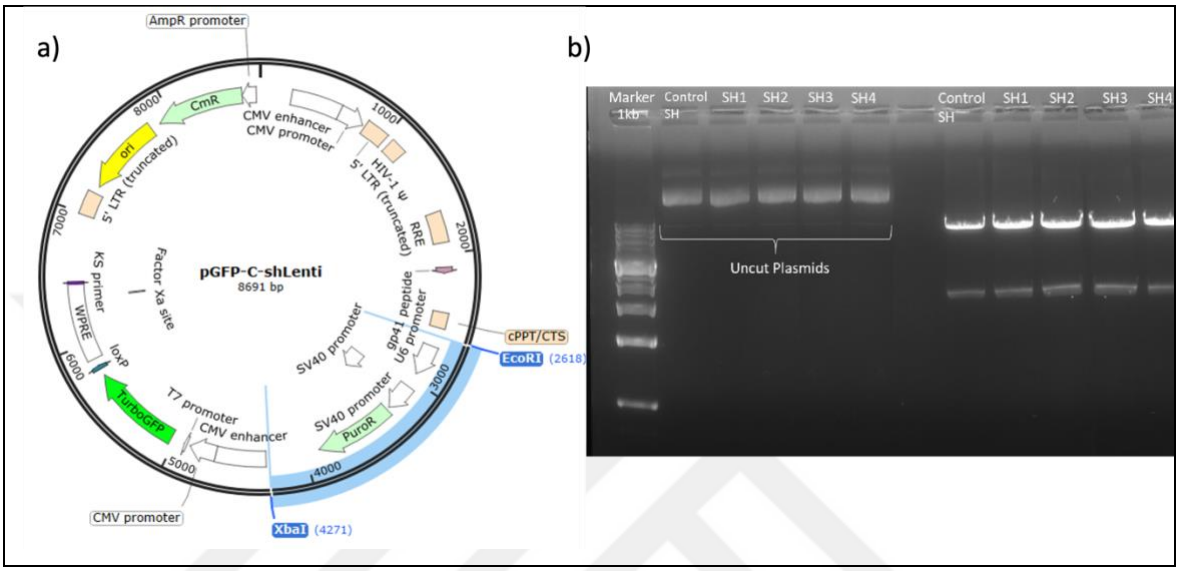

Figure 4.3. Control of restriction digestion. a) Visualization of EcoRI and XbaI enzyme dual-cutting in the SnapGene tool, b) Agarose gel images of enzyme digest products under UV light; Marker: VWR® Amresco EZ-vision® DNA ladder 1 kb.

The results of the cutting products of the plasmids on agarose gel are shown in Figure 4.3b. Accordingly, the bands in the gel were determined as 1653 bp and 7038 bp as expected. This result confirms that the plasmids amplified by bacterial transformation are the same as the main stock plasmids.

4.1.2.2. Lentiviral Transfection of HEK293FT Cells

HEK293FT cells were transfected with shRNA plasmids via the FuGENE HD transfection reagent. Packaging was achieved with second-generation plasmids (VSV-G & dVPR). Transfection efficiency was monitored by GFP fluorescence before collecting the supernatants of the packaged viruses (Figure 4.4). Post-amplification transfection of 4 different plasmid constructs and a scramble (control) plasmid was achieved. It has not yet been decided which plasmid alternative should be preferred at this stage. This was decided by experiments in which post-transduction IL-6R expression was determined.

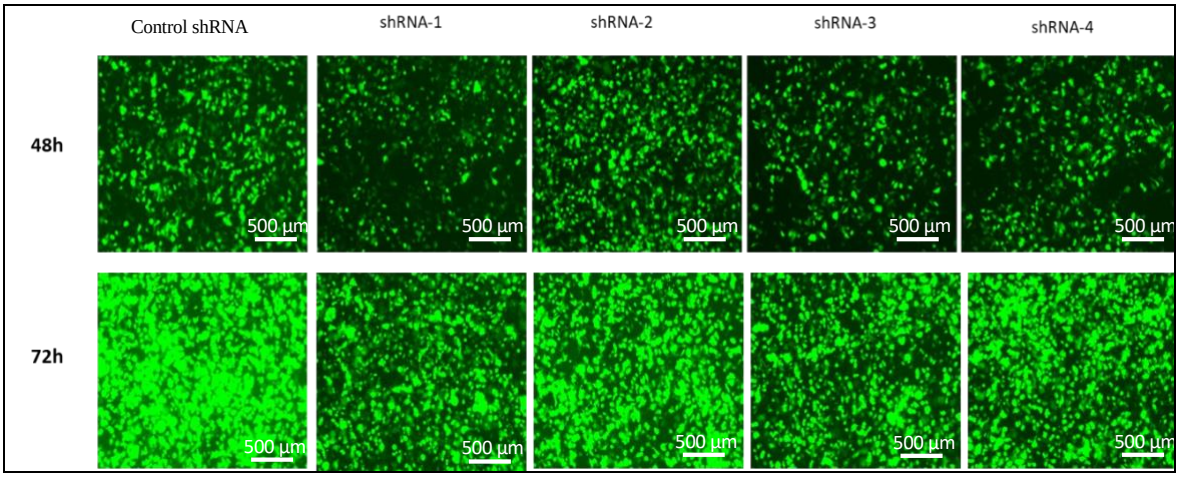

Figure 4.4. GFP fluorescence of HEK293FT cells at 48 and 72 hours after transfection.

4.1.2.3. Selection of chordoma cells after transfection

After transduction of JHC7 and MUG-Chor1 cells, puromycin antibiotic selection was started at 48 hours. A kill curve was generated by treating the cells with puromycin at different concentrations (ranging from 0.1-10 µg/ml) for 14 days (Figure 4.5). It was decided to use 3.5 µg/ml puromycin for the JHC7 cell line and 0.1 µg/ml puromycin for the MUG-Chor1 cell line to use the minimum dose that kills 100% of the cells.

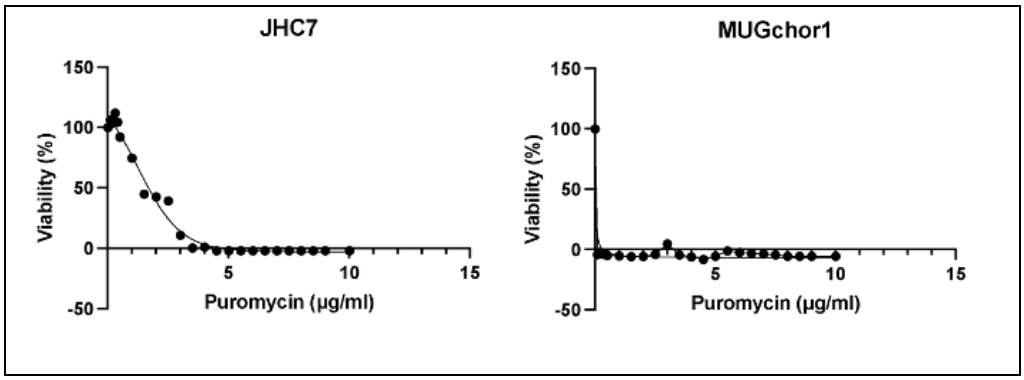

Figure 4.5. Determining the dose of Puromycin.

Selection of cells with puromycin was maintained for 1 week. The cells that remained viable in the population during the selection period are considered to be the cells that integrated the puromycin resistance gene into the cell genome and thus successfully transduced. After this selection, cells were selected by the presence of GFP, another selection mechanism. Successful transduction in chordoma cells requires the integration of the GFP gene in the

plasmid map into the chordoma cell genome and green fluorescence. Based on this selection mechanism, GFP luminescent cells were separated from the total population in the FACS device (Figure 4.6).

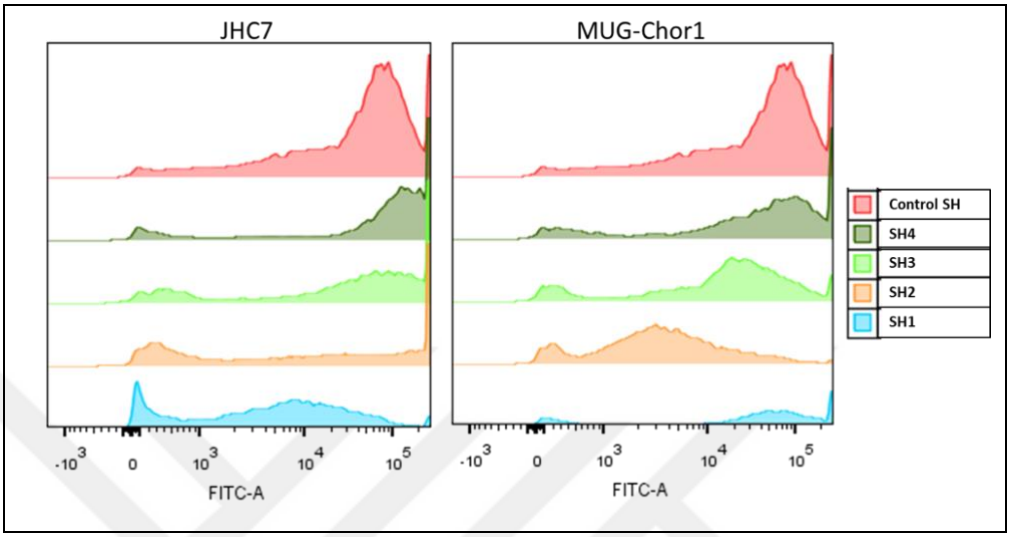

Figure 4.6. GFP (+) populations of chordoma cells transduced with IL6R-shRNA plasmids; JHC7 (Left), MUG-Chor1 (Right).

Using the FACS device, GFP (+) irradiating cells were separated from the main population. Since the percentage of the GFP (+) population was less than 50% in the first separation of cells, this selection was performed twice. Thus, after puromycin selection, cells were selected by GFP (+) cell separation 2 times. This resulted in a pure subpopulation containing more than 80% GFP (+) cells of the total population (Figure 4.6).

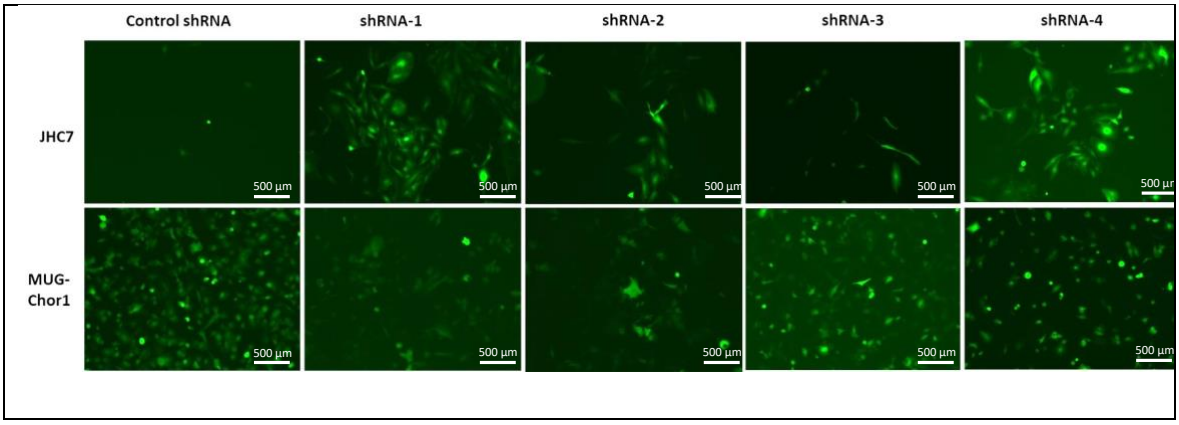

Figure 4.7. Visualization of stable cells after GFP (+) cell sorting. Scale bar 500 µm.

4.1.2.4. Evaluation of IL-6R Gene Silencing

In this part, IL-6R gene silencing was controlled at both mRNA and protein levels. In this way, it was determined which shIL6R construct would be used for transcriptomic and functional experiments.

Control of IL-6R mRNA via qRT-PCR

RNAs isolated from chordoma cells were used to synthesize cDNA. Altered IL6R expression levels in the experimental groups were determined by qPCR using cDNA samples. The effect of 4 different shRNA plasmids on IL-6R mRNA levels in JHC7 and MUG-Chor1 cells compared to the control group is shown in Figure 4.8. *YWHAZ* was used as an internal control gene in the study. In JHC7 cells, compared to the control, IL-6R mRNA level was altered by a -0.62 fold change in the SH3 group, while SH1, SH2, and SH4 were altered by -0,45, +0.04, and -0.07 fold, respectively. In MUGchor1 cells, IL-6R mRNA level was altered by a -1.62 fold change in the SH3 group compared to the control, while SH1, SH2, and SH4 were altered by -1.3, -1.43, and -0.6 folds, respectively. Accordingly, in both cell lines, the plasmid named SH3 was determined as the best targeting plasmid for IL-6R.

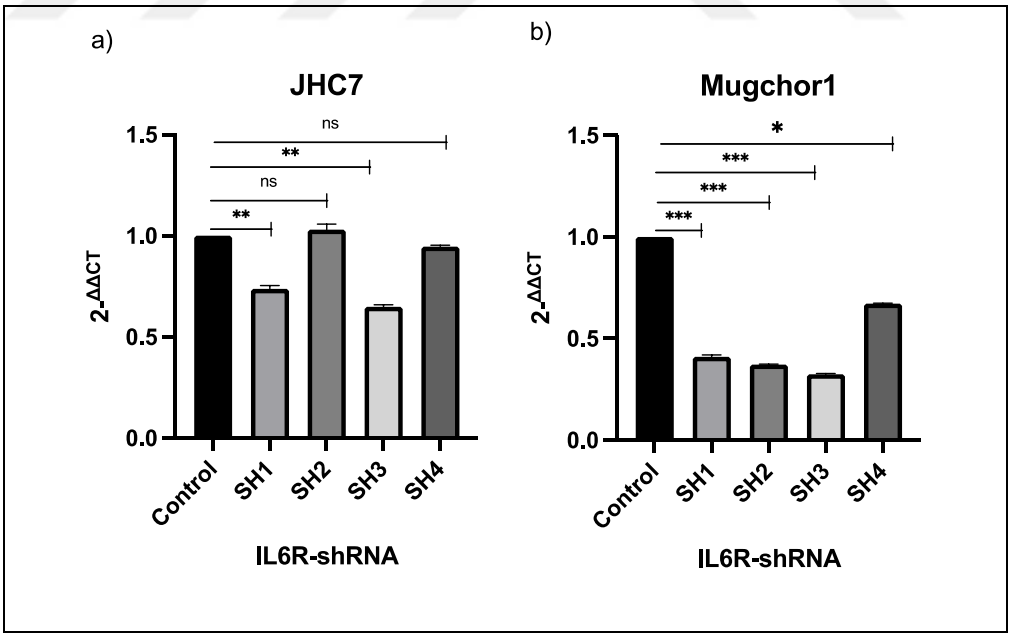

Figure 4.8. Determination of the decrease in IL-6R expression in JHC7 and MUG-Chor1 cell lines. a) IL-6R expression in JHC7 cell line, b) IL-6R expression in MUG-Chor1 cell line.

Control of IL-6R protein via Western blot

The amount of IL-6R protein altered in the cell lines compared to the control groups was determined. GAPDH protein was used as an internal control (Figure 4.9). Compared to the control in JHC7 cells, the IL-6R protein ratio was down-regulated by 70% in the SH1, by 32,5% in the SH2, and by 77% in the SH3 group, while up-regulated by 87% in the SH4 group. In MUGchor1 cells compared to the control, the IL-6R protein ratio was down-regulated by 40% in the SH1, 34% in the SH2, 67% in the SH3, and 52% in the SH4 group. As in qRT-PCR analysis, the SH3 plasmid provided the most efficient silencing in western blotting. After this stage, all subsequent experimental steps were continued with the control group and the SH3 plasmid group that provided the best silencing. Other SH groups with lower silencing efficiency were not used in functional experiments and transcriptome profiling.

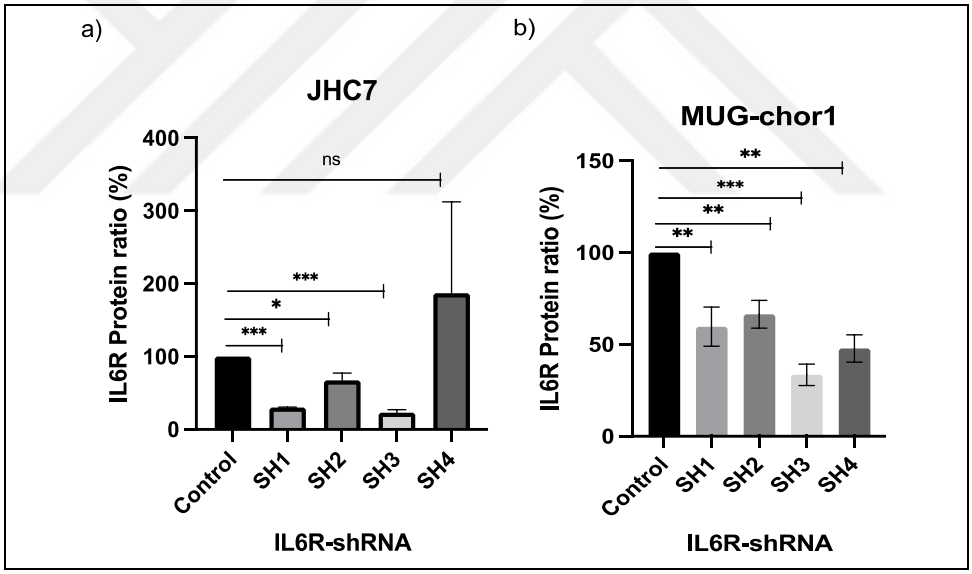

Figure 4.9. Determination of the decrease in IL-6R protein level after transduction of IL-6R shRNAs into cells. a) IL-6R protein level in JHC7 cell line, b) IL-6R protein level in MUG-Chor1 cell line.

4.1.2.5. Evaluation of IL-6R silencing via Tocilizumab

The effectiveness of IL-6R silencing in chordomas was assessed using the FDA-approved drug tocilizumab (TCZ). In JHC7 cells, the TCZ group (10 ug/ml) with the lowest IL6R mRNA level showed a -0.27 fold change compared to the control, while the shRNA group showed a -1 fold change. In MUGchor1 cells, the TCZ group (30 ug/ml) with the lowest

IL6R mRNA level showed a -0.55 fold change compared to the control, while the shRNA group showed a -1.74 fold change. The findings showed that the dose of TCZ that provided the most effective silencing at the mRNA level was not as effective as the shRNAs used in both cell lines. Analysis at the protein level is also necessary to determine the exact efficiency of TCZ silencing of IL6R compared to shRNA.

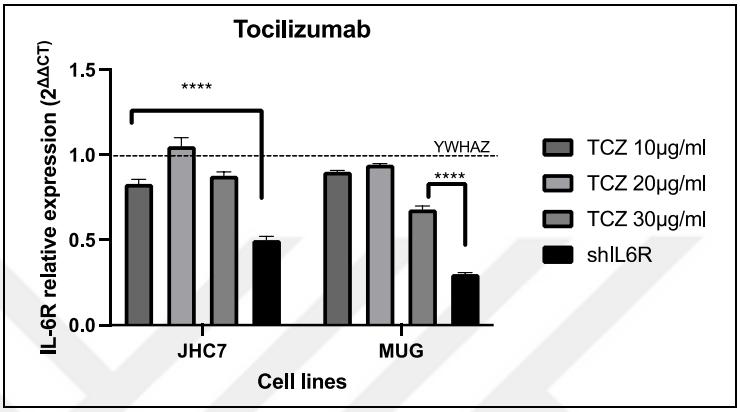

Figure 4.10. Tocilizumab and shRNA comparison for IL-6R silencing efficiency. TCZ (10-20-30 µg/ml) concentrations were applied for 1 week. shRNA was provided by SH3 plasmid to both cell lines. *YWHAZ* was used as an internal control gene.

4.2. DETERMINATION OF TRANSCRIPTOMIC CHANGES

A microarray study was performed for the IL6R silenced-stable cell group and control groups of both cell lines. Before the array, the RNA quality of the experimental groups was determined. RNA Ladder was used as a marker. The 18S and 28S ribosomal RNA (rRNA) of all experimental groups gave distinct bands (Figure 4.11). Thus, it was demonstrated that the RNA qualities were suitable to proceed with the microarray study.

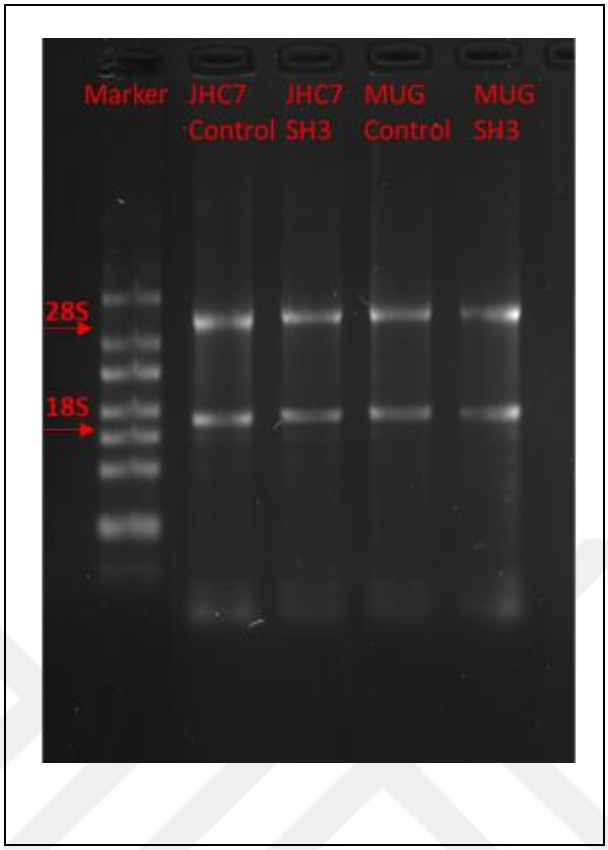

Figure 4.11. Agarose gel image showing RNA quality. Groups to be microarrayed and 28S and 18S rRNA bands of each group.

Microarray analysis was performed repeatedly for the control group and shIL-6R group (IL-6R silenced) of each cell line. In the analysis, 135750 transcripts were detected and analyzed, and the results were expressed as increased/decreased change in IL6R silenced groups compared to control groups. In chordomas used in the study regardless of cell line, 21213 transcripts were considered statistically significant in shIL6R groups compared to control groups. Among these, 4475 transcripts showed a significant increase while 16738 transcripts showed a significant decrease (Figure 4.12).

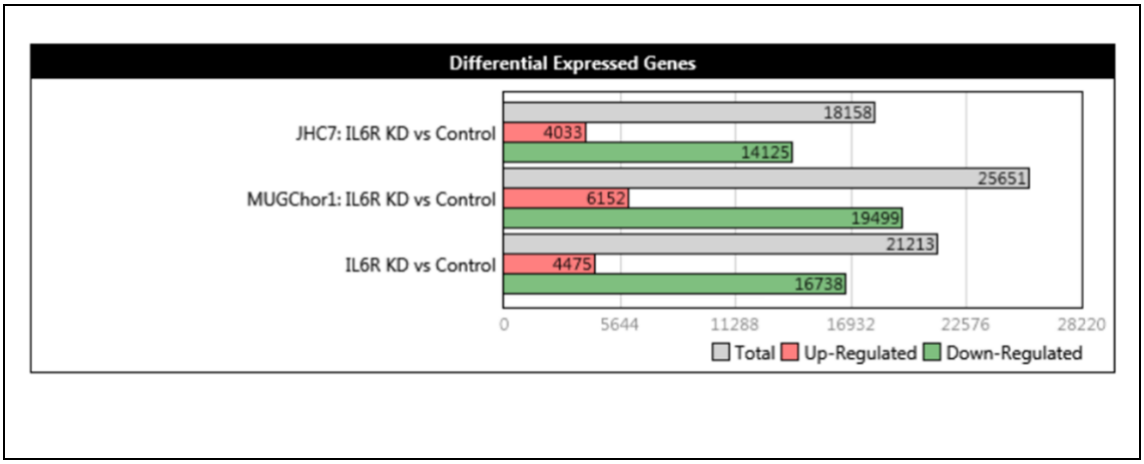

Figure 4.12. Total or cell line-specific increased/decreased ratios of transcripts showing statistically significant changes. IL6R-KD (shIL6R, silenced group), control (control, reference group) groups; up-regulated (increased), down-regulated (decreased) values.

As a result of the microarray study, the distribution of transcripts showing differential expression in IL-6R silenced groups is presented in Figure 4.13.

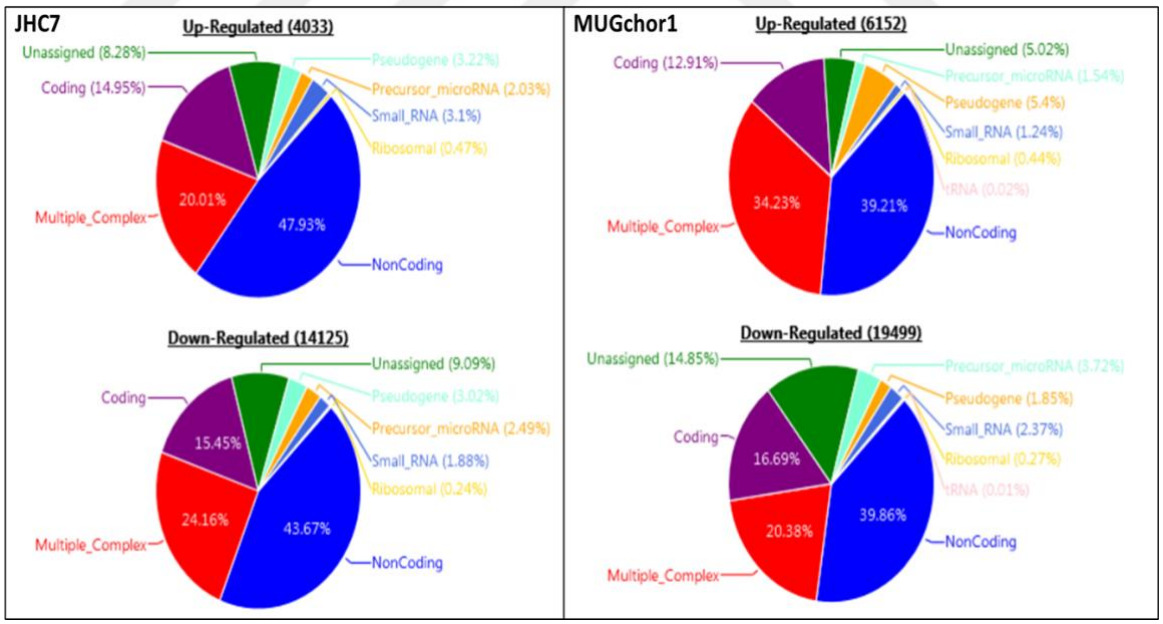

Figure 4.13. Pie charts showing the percentage distribution of transcripts showing differential expression according to their biological function.

Each transcript in the microarray panel corresponds to a point in the volcano scatter plots in Figure 4.13. A volcano plot is a type of scatter plot that describes change in large datasets. In the plot, the X-axis represents the linear fold change of the current state and the Y-axis

represents the -log10 p-value. The graph shows the genes that showed significant change (differential expression) in shIL6R groups compared to control groups (reference groups) for both cell lines; the green population represents the set of genes that significantly decreased and the red population represents the set of genes that significantly increased according to the p-value. The differences of the scatter plots reveal that IL6R silencing induces a different transcriptomic profile in each cell type.

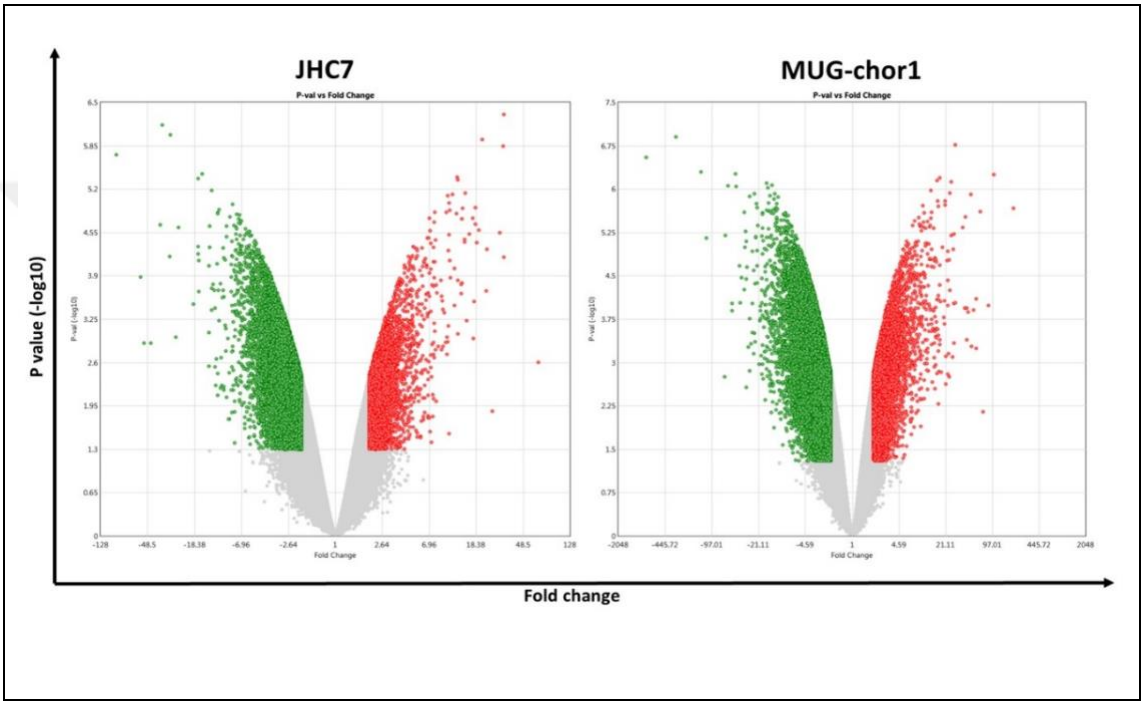

Figure 4.14. Volcano scatter plot of differentially expressed genes with fold change values in -log10 base. The X-axis represents the linear fold change of the current state and the Y-axis represents the -log10 p-value.

It is possible that the genes showing differential expression in shIL6R groups are critical for chordoma and have potential to target. The genes listed in Table 4.2 were generated from transcripts in the coding gene or multiplex category of the Clariom-D microarray. The findings show that the genes listed are genes that have been associated or have the potential to be associated with cancer in the literature.

Table 4.2. List of 5 differentially expressed genes in chordoma cell lines according to the highest/lowest fold change of differentially expressed genes. Upper rows/boxes indicate decreasing and bottom rows/box indicate increasing genes.

Gene Symbol	Fold Change	P value
RNASE2	-760,58	2,20E-07
LDOC1	-289,34	4,82E-05
PCSK2	-140,11	3,45E-06
GPNMB	-91,05	5,37E-07
MAGEC2	-90,53	0,0001
HAPLN1	103,96	0,0251
FOSL1	55,18	4,98E-06
GPC4	37,28	0,0003
MATN2	32,55	0,0011
PPDPF	25,88	0,0002

4.2.1. Functional Enrichment Analysis of the Transcriptome with Differential Expression

WikiPathways, an analysis tool of the TAC software, is a functional bioinformatics analysis tool that computes the probability that genes and pathways are affected by changing expression. Genes/pathways whose expression changed as a result of IL-6R gene silencing were identified with this analysis. This analysis was determined by the most affected genes according to their number in the pathway. The 10 pathways that were determined to be the most affected and the 10 genes (5 increasing/5 decreasing) that showed the most change in those pathways are listed (Table 4.3).

Table 4.3. Pathways most altered in common in IL-6R silenced cells compared to control in both cell lines according to TAC/WikiPathways analysis. Up gene list: 5 genes with the most increased expression, Down gene list: 5 genes with the most decreased expression.

Pathways	Up Gene List	Down Gene List
VEGFA-VEGFR2 signaling	ROCK, PIK3R2, ITGAV, MAPKAPK2, CAPN2	ABCF2, MAPK14, FRS2, PTK2, TPCN2
Malignant pleural mesothelioma	TCF7L1, CTGF, PLCB4, PHC1, HCFC1	KDM6A, BTC, ED, EZH2, LAMC1
PodNet: protein-protein interactions in the podocyte	ENAH, F3, FOXC2, IGFBP7, CUX1	ZHX2, TNS2, RAB4B, PSENEN, VCL
Focal adhesion: PI3K-Akt-mTOR signaling pathway	LAMB1, PIK3R2, TNC, ITGAV, LAMA2	PIK3CA, ITGB4, PTK2, ITGB2, COL5A2

PI3K-Akt signaling pathway	LAMB1, PIK3R2, TNC, ITGAV, LAMA2	PIK3CA, ITGB4, COL6A3, PTK2, LAMA4
Nuclear receptors meta-pathway	SOD3, SERTAD2, G6PD, SLC2A13, FASN	CES1, SRGN, IL12A, SLC2A11, TNFAIP3
IL-18 signaling pathway	IRAK1, CYCS, IL18, BAX, IER3	IMP3, CL3, IL18BP, MMP3, MMP14
Endothelin pathway	WNK1, CCND1, TPM4, PLCB1, FOXK2	BCAR3, ABHD3, FLNB, COL7A1, VCAN
Focal adhesion	CAPN2, ILK, LAMA2, ITGB8, FYN	COL1A1, MET, PTK2, MAP2K1, ERBB2
MAPK signaling pathway	ARRB2, ARAF, FLNA, MAPKAPK2, HSPB1	CD14, BDNF, MAPK14, MAP2K5, MAP2K1

The numerical distribution of the pathways whose expression was altered is presented as a Venn diagram in Figure 4.15. These are indicated by grouping the number of pathways found to be altered in common in both cell lines. Accordingly, there were 186 common genes showing increased expression in JHC7 and MUG-Chor1 cell lines. There were 884 common genes showing decreased expression in both cell lines.

Figure 4.15. Numerical distribution of enriched common pathways among cell lines. a) Venn diagram representing genes with significantly increased expression/UP, b) Venn diagram representing genes with significantly decreased expression/DOWN.

The study aimed to identify genes that may be effective in chordoma pathogenesis focused on IL-6 signaling. Accordingly, transcripts whose expression changed significantly changed in shIL6R groups compared to control groups in both JHC7 and MUG-Chor1 cells were analyzed. When evaluating the altered transcriptomic profile, all genes with $p<0.05$ and an absolute fold change of more than 2 were considered statistically significant. DAVID (The Database for Annotation, Visualization, and Integrated Discovery) Database was used for functional enrichment analysis of genes with significant changes in expression. For this purpose, these genes were evaluated according to the biological processes they impact, in addition to the genes whose expression altered most significantly. Accordingly, the prominent pathways and cellular function definition were determined in the analysis performed by using the genes that showed a significant increase or decrease (up/down) in the shIL6R groups compared to the control groups in the study, regardless of the cell line. Among these, the 15 pathways with the highest significance (p-value) for both up/down pathways were filtered. Table 4.4 lists the prominent cancer-related pathways among these pathways. GO terms, KEGG, and Reactome pathway analysis were considered in the analysis performed using the DAVID database.

Table 4.4. List of cancer-associated pathways analyzed using co-increasing or co-reducing gene lists in chordoma cells.

GOterm Category / UP	Term/Pathway	PValue	Genes
Reactome_pathway	Metalloprotease DUBs	1.9E-5	HIST1H2AK
Reactome_pathway	HDACs deacetylate histones	7.4E-4	HIST1H2AK
Biological process	Regulation of cell migration	0.001	LAMA2, TMSB15B, TNC, FGF2
Reactome_pathway	UCH proteinases	0.001	HIST1H2AK
KEGG_pathway	Necroptosis	0.002	HIST1H2AK
Biological process	Positive regulation of angiogenesis	0.004	DDAH1, SERPINE1, HSPB1, PRKCA, FGF2
GOterm Category / DOWN	Term/Pathway	PValue	Genes
Molecular function	Protein homodimerization activity	8.8E-4	TENM1, GBP5, EXD2, ZHX2, DGKD,…
Biological process	Regulation of transcription from RNA polymerase II promoter	0.002	ZNF793, ZNF573, ZNF790, PHF20, ZNF518B,…

Molecular function	Translation initiation factor binding	0.005	GLE1, TBL2, FMR1, EIF3F
Biological process	Ubiquitin-dependent ERAD pathway	0.007	NPLOC4, EDEM1, MAN1A1, DNAJB14, ANKZF1,…
Molecular function	Cytokine receptor activity	0.012	GHR, IL1RL1, LIFR, OSMR, IL6R
Cellular component	Cytoplasmic stress granule	0.012	RPTOR, ATXN2L, CELF1, FMR1
Biological process	Regulation of transcription, DNA-templated	0.012	ZNF793, ZNF573, ZNF790, PHF20, ING1,…

Another analysis with the DAVID database was performed separately for each cell line. The aim was to identify common increased or common decreased pathway/function in both cells. The genes with increased and decreased expression in JHC7 and MUG-Chor1 cell lines were listed and their functional roles were interpreted through bioinformatic analysis (Table 4.5). Accordingly, it was determined that genes with increased expression in both cell lines were associated with the Hippo signaling pathway (KEGG), while genes with decreased expression affected the nucleus and golgi membrane and cellular components (Gene Ontology).

Table 4.5. Pathways and GO terms common to both cell lines. $p<0.05$ was generated by filtering.

Cell line	Category	Upregulated Term/Pathway	P-Value	Genes
JHC7	KEGG_pathway	Hippo signaling pathway	0.025	TGFB3, WWC1, SERPINE1, BMP8B, WNT16, BMP6, BMP5, GLI2,…
MUG	KEGG_pathway	Hippo signaling pathway	8.74E-7	YWHAE, CRB1, YWHAB, LEF1, SERPINE1, PPP2R2A, FGF1, ACTB,…
Cell line	GOTERM Category	Downregulated Term/Pathway	P-Value	Genes
JHC7	Cellular Component	Nucleus	8.21E-5	-
JHC7	Cellular Component	Golgi membrane	3.515E-4	-
MUG	Cellular Component	Nucleus	4.09E-13	-
MUG	Cellular Component	Golgi membrane	6.35E-6	-

Another tool applied through the DAVID database is the analysis of GO terms. The Gene Ontology (GO) knowledge base is a computational analysis tool that provides information about the functional attributes of genes. GO term enrichment is a technique for interpreting gene clusters using the GO classification system in which genes are assigned based on their functional properties [77]. According to GO Terms analysis, common decreasing functions were identified in both cells.

4.2.2. Confirmation of Microarray Study

As a result of the microarray study, genes whose expression changed differentially in the IL-6R silenced groups compared to the control were identified. Among these genes, two genes (*GSTM3* & *MMP1* for JHC7 and *VIM* & *ZEB1* for MUG-Chor1) that were significantly changed in JHC7 and MUG-Chor1 cell lines were selected. In JHC7 cells, compared to the control, *GSTM3* mRNA level was increased by a +2 fold change in the shIL6R (SH3) group, while *MMP1* mRNA level was increased by -1.5 fold, respectively. In MUG-Chor1 cells, compared to the control, *ZEB1* mRNA level was increased by a +2.3 fold change in the shIL6R (SH3) group, while *VIM* mRNA level was increased by +0.85 fold, respectively. The mRNA levels of the selected genes were checked by qRT-PCR and confirmed to be microarray consistent.

Table 4.6. Genes indicated are those whose expression changed significantly in the microarray.

JHC7 shIL6R vs. Control	Fold change	P value	Mugchor1 shIL6R vs. Control	Fold change	P value
MMP1	-3.7	0.0197	VIM	-3.7	0.0197
GSTM3	6.93	0.0140	ZEB	6.93	0.0140

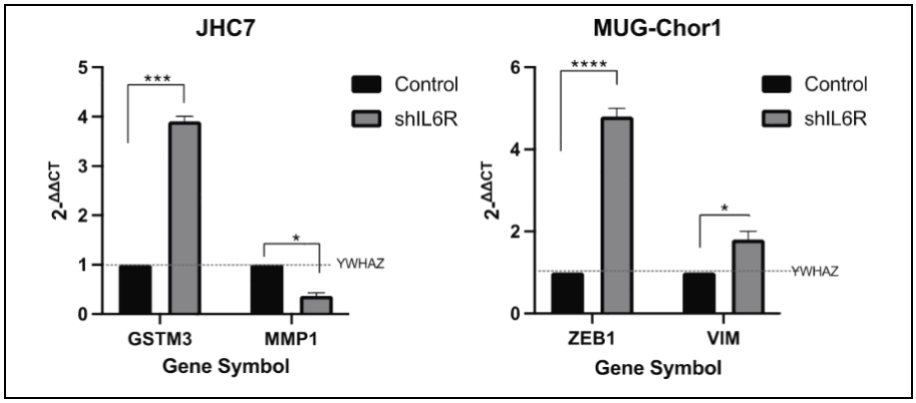

Figure 4.16. Confirmation experiment of the microarray study. qRT-PCR findings, *YWHAZ* was used as internal control.

4.3. EFFECTS OF IL-6R GENE KNOCK-DOWN ON THE FUNCTIONAL PROPERTIES OF CHORDOMAS

IL-6R silenced cell line (JHC7-SH3) and JHC7 Control group were used for JHC7 cell line. For MUG-Chor1 cell line, IL6R silenced cell line (MUGchor1-SH3) and MUG-Chor1 Control group were used. In addition, functional experiments were performed with a total of 4 groups for each cell line, including two more experimental groups formed by applying recombinant human IL-6 protein (Prospec, Cat no: #cyt-213) to these two cell groups. The dose and period of IL-6 protein applied were determined accordingly to literature findings and preliminary studies. Accordingly, it was applied at a concentration of 50 ng/ml in both cell lines. All experiments were performed in 3 replicates.

4.3.1. Migration and Invasion Assays

Results obtained from experiments performed with the Boyden chamber protocol showed that the migration and invasion capacities of the IL-6R gene silenced groups were decreased compared to the control group (Figure 4.17). In JHC7 cells, the migrated cell ratio was downregulated by 42% in the shIL6R compared to the control group. In the IL6-treated JHC7 groups, the migrated cell ratio was down-regulated by 18% in the shIL6R w/IL6 compared to the control w/IL6 group. In MUG-Chor1 cells, the migrated cell ratio was downregulated by 4% in the shIL6R compared to the control group. In the IL6-treated MUG-Chor1 groups, the migrated cell ratio was down-regulated by 15% in the shIL6R w/IL6 compared to the Control w/IL6 group. In JHC7 cells, the invaded cell ratio was downregulated by 13% in the

shIL6R compared to the control group. In the IL6-treated JHC7 groups, the invaded cell ratio was up-regulated by 13% in the shIL6R w/IL6 compared to the Control w/IL6 group. In MUG-Chor1 cells, the invaded cell ratio was downregulated by 30% in the shIL6R compared to the control group. In the IL6-treated MUG-Chor1 groups, the invaded cell ratio was down-regulated by 23,5% in the shIL6R w/IL6 compared to the Control w/IL6 group.

The recombinant IL-6 protein applied exogenously to the culture medium did not show a significant and pronounced effect on the migration and invasion capacities of the cells. Analysis of the number of migrating cells showed that the migratory potential of JHC7 cells was higher than that of MUG-Chor1 cells.

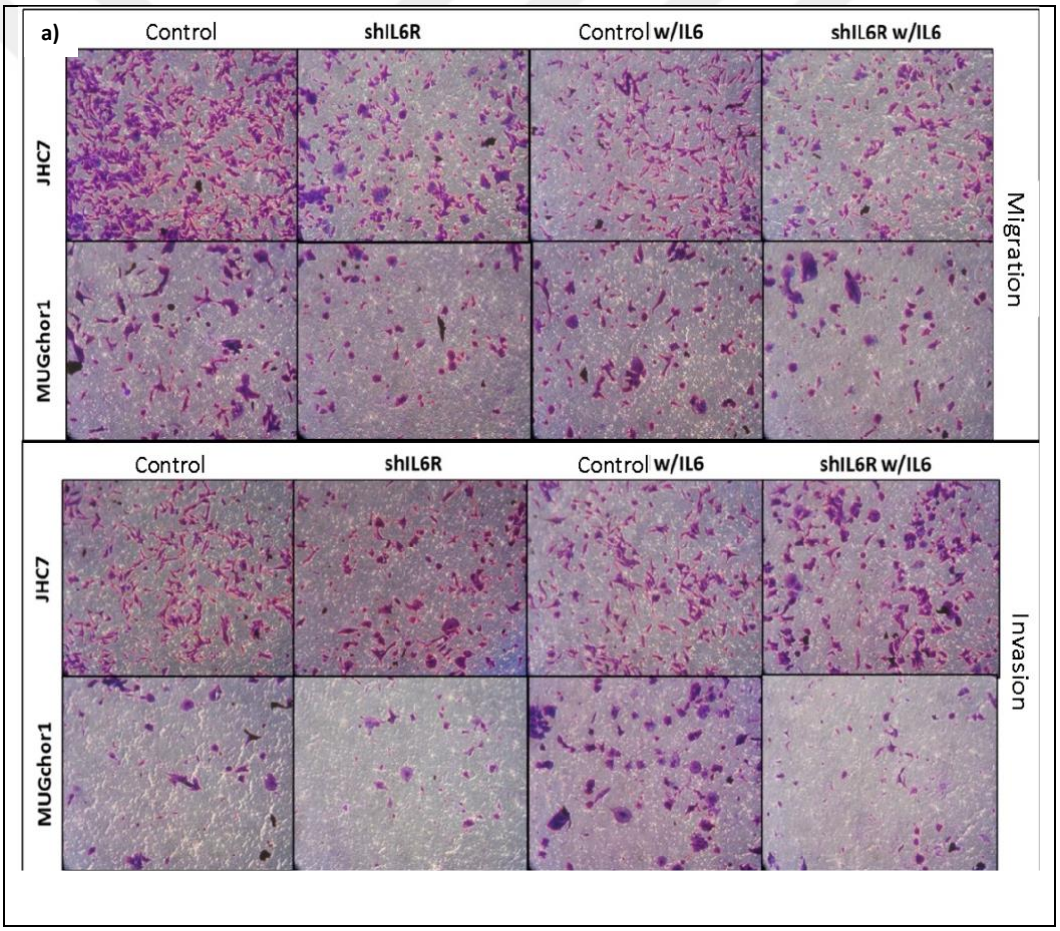

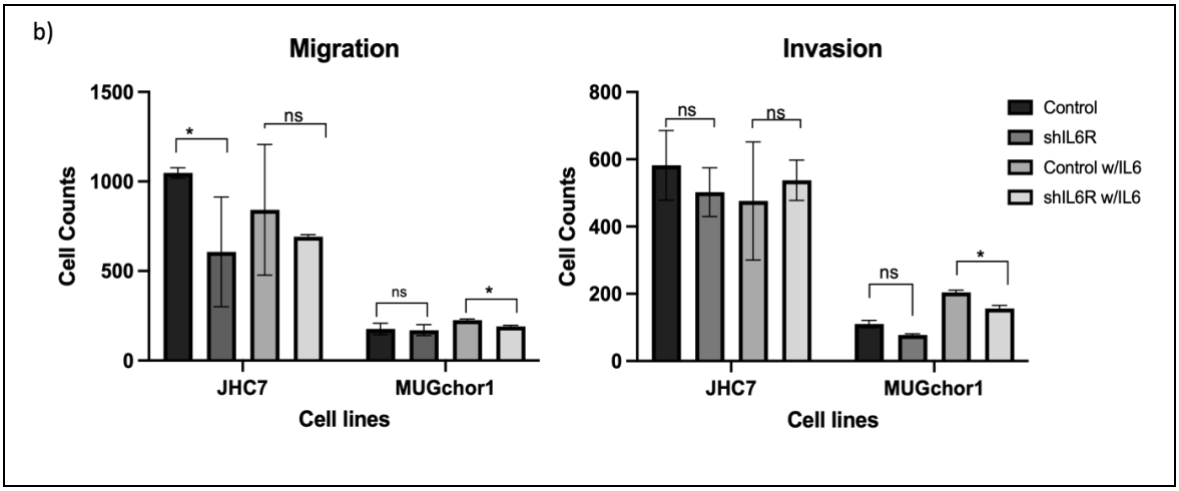

Figure 4.17. Determination of the effects of IL6R signaling on the migration and invasion capacity of chordoma cells. a) Microscope (10X magnification) images of crystal violet stained cells representing the experimental groups, b) Column graph representation of the results obtained by analysis of repeated experiments.

4.3.2. Tumorsphere Formation Assay

On the 9th day of the experiment, the spheres in the control w/IL6 group in the JHC7 cell line turned into a form whose center parts darkened. This stage was determined as the morphologically ready form to end the experiment. Therefore, the experiment for JHC7 cells was terminated at the end of the 9th day. On the 9th day of the experiment, the JHC7-shIL6R (JHC7-SH3) group exhibited a higher number and larger size of spheres compared to the control group. IL-6 treated JHC7 groups were more significantly affected by IL-6 treatment compared to other functional assays performed. Accordingly, IL-6 treated JHC7 cells caused an increase in the number and size of spheres.

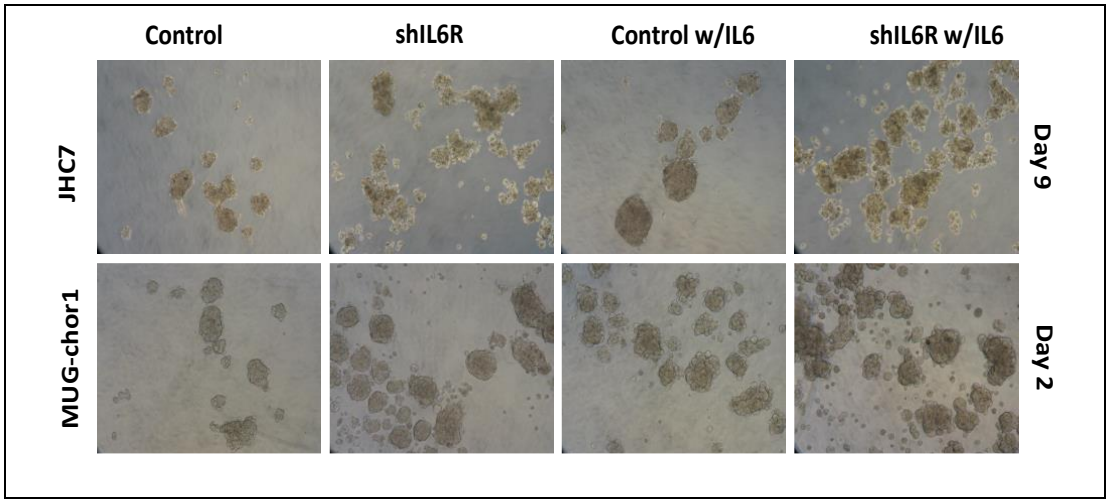

Figure 4.18. Microscope (10X magnification) images of tumor spheres formed in JHC7 and MUG-Chor1 cell lines.

The spheres of the MUG-Chor1 shIL6R (MUGchor1-SH3) group started to form blackened spheres at the end of the 2nd day, which were quite large and had an increased population of dead cells. Therefore, it was decided to terminate the experiment based on this group at the end of day 2. Comparison between groups was provided for other MUG-Chor1 cells during this period. Tumor sphere formation potential was higher in the IL-6R silenced group in MUG-Chor1 cells than in the control group. Moreover, IL-6 treatment increased the number and size of spheres in MUG-Chor1 cells and positively affected the tumor sphere formation capability. As compared to other functional tests carried out on MUG-Chor1 cells, sphere formation seems to be more strongly impacted by IL-6 treatment.

4.3.3. Scratch Assay

According to the findings obtained from the scratch experiment, the Control group, which was the first group to achieve complete closure in the JHC7 cell line, reached 100% closure at the scratch line on day 5 (Figure 4.19a). On the 5th day of the experiment, the 'Control w/IL6' group was the second group to reach complete closure. The group with the latest scratch closure was IL-6 treated shIL6R (shIL6R w/IL6). In the MUG-Chor1 cell line, the Control group, which was the first group to achieve complete closure, reached 100% closure on the 11th day (Figure 4.19b). The shIL6R group had the latest scratch closure in MUG-Chor1 cells. When the experiment was evaluated for both cell lines, silencing of the IL6R gene slowed down the rate of cell migration and thus the rate of scratch closure. In addition,

IL-6 treatment of control and shIL6R groups did not cause a significant change in cell motility.

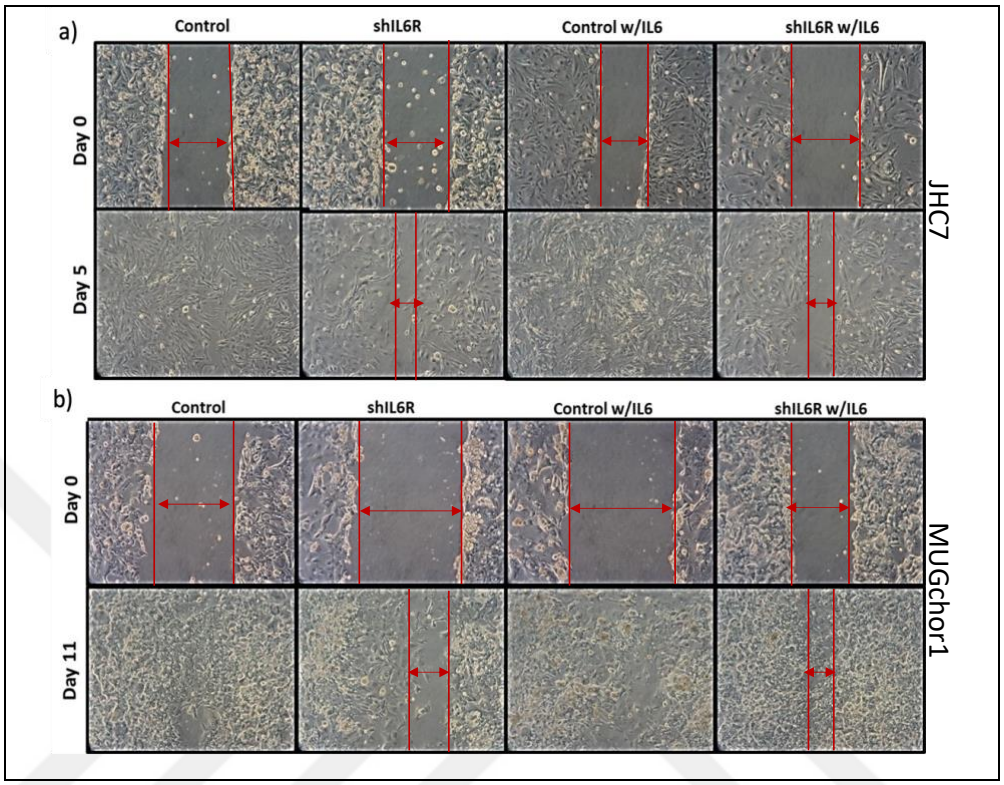

Figure 4.19. Microscope (10X magnification) images of the beginning and end of the scratch closure experiment. a) Experimental images for the JHC7 cell line, b) Experimental images for the MUG-Chor1 cell line.

4.3.4. The Effects of IL-6R Knock-down on CSC and EMT Markers

In chordoma cell lines, IL-6R silencing was also assessed in terms of CSC and EMT markers (Figure 4.20). The results show that *NANOG*, *SOX2* and *VIM* are genes that change in the same manner throughout the two cell lines. In both chordoma cell lines, the relative expressions of *NANOG* and *SOX2* decreased while the relative expression of *VIM* increased. The relative expression changes for *OCT4 (POU5F1)* and *CDH2 (N-CAD)* among chordoma cell lines revealed opposing trends. *OCT4* and *CDH2 (N-CAD)* relative expressions were increased in JHC7 cell line and decreased in Mugchor1 cell line.

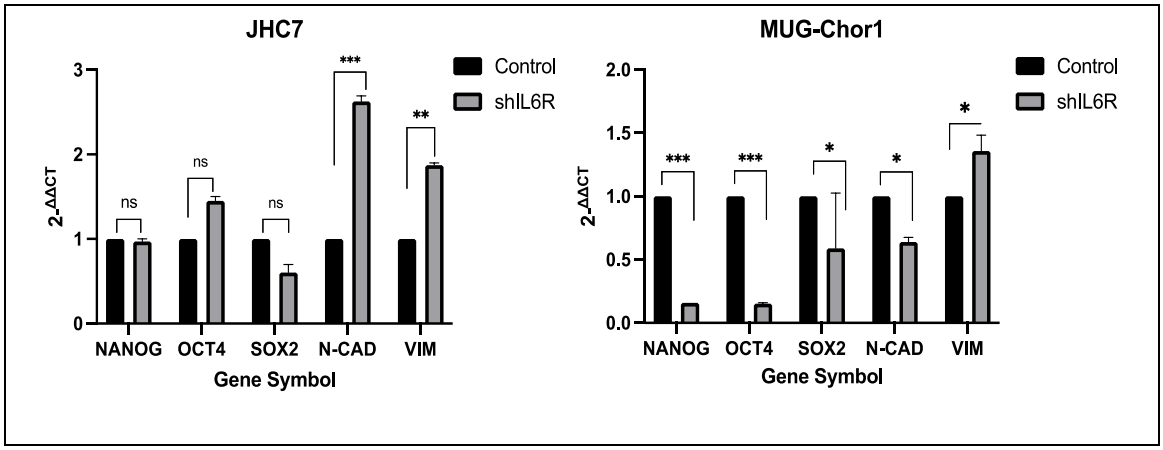

Figure 4.20. *NANOG, OCT4, SOX2, CDH2* and *VIM* genes were used as CSC&EMT markers. Statistical analyses were performed by t-test ($p<0.05$), calculations and graphs were prepared with GraphPad-Prism program. *YWHAZ* was used as an internal control gene in the study

In JHC7 cells, compared to the control, *NANOG* and *SOX2* mRNA levels were decreased by -0.04 and -0.74 fold change in the shIL6R (SH3) group, while *OCT4*, *N-CAD*, and *VIM* mRNA levels were increased by +0.53, +1.4, and +0.9 fold, respectively. In MUG-Chor1 cells, compared to the control, *NANOG*, *OCT4, SOX2*, and *N-CAD* mRNA levels were decreased by -2.64, -2.74, -0.74, and -0.64 fold change in the shIL6R (SH3) group, while *VIM* mRNA level was increased by +0.43 fold, respectively.

5. DISCUSSION

Studies have demonstrated that the IL-6 cytokine promotes the growth of tumors and is crucial for apoptosis resistance. This thesis was the first to investigate the effectiveness of IL-6 signaling in chordomas. To achieve this, the signaling was investigated with particular attention on IL-6R, one of the molecules that provides the IL-6 signaling activity for the present research.

Following initial investigations using chordoma cell lines in our lab, it was found that chordoma cell lines triggered to a more aggressive phenotype also exhibited an enhanced IL-6 signaling. Another early investigation found that chordomas had a considerably greater amount of IL-6 cytokine when comparing the medium content of healthy (Nucleus pulposus) and chordoma cells. With this knowledge in hand, we decided to use a down-regulation/silencing (knockdown) strategy to study IL6 signaling in chordoma cells.

Basically, three molecules need to work together for IL6 signaling to be active. These are gp130 (IL6ST), IL-6, and IL-6 receptor [41–43]. The pleiotropic molecule IL-6, which is expressed in numerous tissues and is crucial to the immune response, has both pro- and anti-inflammatory properties [78, 79]. Owing to these crucial functions, IL-6 was not the target molecule preferred for signaling efficiency. The gp130 molecule is crucial for development, hematopoiesis, cell survival, and growth even though it is known as the IL-6 receptor's signaling subunit. Additionally, the gp130 molecule acts as a β-cytokine receptor for leukemia inhibitory factor (LIF), ciliary neurotrophic factor (CNTF), IL-11, IL-27, oncostatin-M (OSM), and cardiotrophin-like cytokine (CLC) (80). It has been established in the literature that the deletion of gp130, which is present in many immune system cells and organs, causes embryonic death in mice [75]. For these reasons, we focused on the IL-6 receptor (IL-6R) molecule in the investigation of IL-6 signaling.

The goal of the study's initial stage was to knock-out the IL-6R gene. CRISPR/Cas9&HDR plasmids customized targeting the IL-6R gene were used for this objective. Nevertheless, following CRISPR-based transfection, chordoma cells were dead. The control group, however, maintained its viability. The experimental groups did not yield any successful results, even with many transfection alternatives. Just a small viable colony could be established in transfection investigates conducted on easily transfected HEK293FT cells. These findings indicate that cell viability can be affected by IL-6R gene deletion (knock-

out). The small number of alive HEK293FT cells disables the confirmation of IL-6R gene knock-out. Therefore, the pattern of IL-6R gene deletion inducing cells to apoptosis was examined. The results confirmed that deletion of the IL-6R gene caused cell death (Figure 4.2). After this stage, it was decided to apply a silencing method rather than completely delete the IL-6R gene to maintain cell viability. In the literature, an *in vitro* knock out strategy is not preferred for the IL-6R gene. Instead, the siRNA/shRNA approach is frequently used. However, the IL-6R gene was frequently deleted in *in vivo* experiments [81–84]. This preference may be due to the fact that the absence of IL-6R is tolerable in metabolism but not in cell culture conditions.

The shRNA technology was used to target the IL-6R molecule to decrease or suppress IL-6 activity. The selection of shRNA for the utilized RNA interference technique required stable silencing activity. Since chordoma cell lines have extremely long doubling periods, it would not be appropriate to apply an unstable silencing strategy for transcriptome analysis or functional investigations [85, 86].

Our study also evaluated Tocilizumab (Actemra); a monoclonal antibody used clinically for IL-6R inhibition. Therefore, it is possible to claim that Tocilizumab, which is used to treat COVID-19, various types of cancer, and inflammatory diseases, is unable to completely suppress IL-6R [87–89]. The receptor IL-6R has two isoforms that are both soluble and membrane-bound. The shIL6R construct used in our study was designed to target both isoforms. In the literature, Prenissl et al. argue that Tocilizumab is not effective for the sIL-6R isoform [90]. Prenissl's argument may explain the IL-6R inhibition efficiency of Tocilizumab in our study. In our study, Tocilizumab and shIL6R (SH3) were evaluated at the mRNA level for the efficiency of IL6R silencing in chordoma cell lines. To determine the effect of Tocilizumab in the chordoma cell lines, IL-6R protein level should also be examined and its effect in functional assays should also be determined.

Post-transduction selection is independent of the plasmid's target site success or silencing efficiency. The success of these selections reflects the efficiency of shRNA plasmids during packaging, transfection, and transduction. In this research, the mRNA and protein levels transcribed from the IL6R gene were assessed to evaluate the IL-6R gene-targeted silencing efficacy of shRNA plasmids. Instead of utilizing the single target plasmid construct of the shRNA method, four different alternative plasmid constructions (SH1, SH2, SH3, and SH4) were used to target IL-6R. These plasmids were designed to target different regions within

the IL-6R gene. In our study, the plasmid structure that provides the most efficient IL-6R silencing (by analyzing mRNA and protein levels) without negatively affecting cell viability was preferred.

The results of this study's functional assays showed that, in both cell lines, the shIL6R (IL-6R silenced) group of cells had less capacity for invasion and migration than the control groups. This demonstrates that the ability of IL-6 signaling to boost cell motility and the tendency to metastasis is diminished upon silencing [45, 91, 92]. The cells' ability for migration and invasion did not dramatically change when recombinant IL-6 was added to the culture medium. This suggests that the suppression of IL-6 receptor activity is not tolerated by other mechanisms and the increase in IL-6 in the medium does not significantly contribute to cell motility through alternative pathways. The chordoma cell lines used in our project were isolated from tumor samples that occurred in the sacral region of the axial skeleton and had different metastasis/recurrence characteristics [12, 93]. It is therefore believed that the two chordoma cell lines in the study differ from one another in terms of their clinicopathologic traits (primary/relapse).

Another functional experiment used to evaluate cell migration was the scratch assay. Our hypothesis was supported by the results, which indicated that in both cell lines, shIL6R groups had lower scar closure ability/cell migratory capability than control groups. Recombinant IL-6 treatment did not show a significant increase in the migratory ability of the cells. When scratch closure, migration, and invasion experiments based on cell motility are evaluated together, the presence of IL-6 in the culture medium did not provide a significant change in the migratory ability of chordoma cells. This may be due to the fact that IL-6 added to the culture medium did not have sufficient effect on the downstream pathways that would contribute to the functional properties of the cells [94, 95].

According to the tumor-sphere formation assay findings, an increase in the tumor-sphere formation ability of shIL6R experimental groups was observed in both cell lines compared to the control groups. There are studies reporting that cancer stem cell potential, EMT orientation and tumor sphere formation are promoted by IL-6 expression. However, in our study, we obtained findings contrary to the literature on this issue. Future research ought to investigate this matter about chordoma. Furthermore, compared to the non-IL6-treated groups, there was a notable increase in tumor-sphere formation in the groups treated with recombinant IL-6. This might result from exposure to IL-6 causing enhanced proliferation.

Zhou et al. reported that the capacity to form a tumor-sphere form depends on size and quantity and that the large sphere form is related to the number/proliferation of cells [96].

The first study of cancer stem cells in chordomas was by Aydemir et al., who reported the presence of high *NANOG, OCT4*, and *SOX2* expression in chordoma CSCs [97]. Furthermore, Li et al. suggested that *SOX2* could be used as a biological target in chordoma [98]. In another study, Lozano et al. identified *SOX2* as a chordoma biomarker [99]. *NANOG* is defined as a CSC marker that shows high expression in different cancer types [100, 101]. Studies have shown that the *NANOG* induces traits such as invasion, metastasis, stemness, self-renewal, and chemoresistance through the use of the PI3K/Akt, JAK/STAT, and Wnt/β-catenin pathways [102–104]. The *OCT4* (octamer-binding transcription factor 4) transcription factor is a Yamanaka factor that promotes the maintenance of CSC properties. *OCT4* can affect chemotherapy resistance, metastasis, and the EMT process in addition to maintaining stemness [105–107]. *OCT4* is known to regulate many of these processes via the Wnt pathway, just as *NANOG* [106–108]. As a transcription factor, SO*X2* controls a variety of physiological functions, including homeostasis, reprogramming, and stem cell self-renewal. Several cancer types exhibit dysregulated *SOX2* expression. Overexpression of *SOX2* is linked to poor survival in cancer. *SOX2* is positively correlated with proliferation, survival, invasion/metastasis, and cancer stemness [109–112]. These pathways are crucial in the relationship between IL-6 and cancer and have an important role in IL-6 signaling. Therefore, an alteration in these markers' expression is crucial to this investigation.

In our investigation, *NANOG* and *SOX2* expression decreased in the IL-6R gene silenced groups in both chordoma cell lines. The fact that the expressions of these genes, which are highly expressed in different cancer types, decreased with the suppression of IL-6 signaling in chordoma was a result correlated with the prediction of the study. In our study, *OCT4* expression in IL-6R silenced groups showed different orientations among chordoma cell lines. Accordingly, the *OCT4* level increased in JHC7 cells, while it decreased in MUG-chor1 cells. Based on this information, it is possible that the high *OCT4* expression in the IL-6R silenced chordoma cells contributed to their ability to develop more and larger spheres in JHC7 cells in the tumor-sphere formation assay.

Epithelial cell markers decrease during epithelial-mesenchymal transition (EMT), whereas mesenchymal cell markers like *Vimentin* and *N-cadherin(CDH2)* are expressed more often [71, 113–115]. In this investigation, we examined the EMT orientation of IL-6R silenced

chordomas through *CDH2* and *Vimentin*. The *CDH2* relative expression in IL-6R silenced cells showed different orientations among chordoma cell lines. Accordingly, *CDH2* expression increased in JHC7 cells, while it decreased in MUG-chor1 cells. *Vimentin* expression was increased in both IL-6R silenced chordomas cell lines. *CDH2* is a cell adhesion glycoprotein that provides cell-cell connection. Its elevated expression has been reported in many cancer types including chordoma [116–118]. The different orientation of the expression level of this gene in the two IL-6R-silenced chordoma cell lines, like *OCT4*, may be related to the different origin/relapse status of the cell lines. Furthermore, it's possible that, like the *OCT4*, the high expression of *CDH2* in IL-6R silenced JHC7 cells affects their ability to generate tumor-spheres. In the literature, Yuan et al. reported that JHC7 and MUG-chor1 cells showed opposite EMT profiles as a result of selective suppression, like *OCT4* and *CDH2* profiles in this study [119]. *Vimentin* expression was increased in IL-6R-silenced chordomas. *Vimentin* shows increased expression in many cancer types and positively affects proliferation and migration [120]. However, several studies have reported that *Vimentin* downregulation triggers drug resistance and CSC phenotype in cancer [121]. High expression of *Vimentin* is frequently associated with a poor prognosis in the literature [122–125]. We found that, in contrast to what occurs for malignancies, there was an increase in vimentin levels in IL-6R-silenced chordomas. Additional investigation is required to understand why there is an increase in vimentin expression in chordomas when IL-6R is silenced.

Gene expressions altered by IL-6R silencing in chordoma cell lines were determined by Clariom D total transcriptome microarray. The transcriptomic changes induced by silencing in both chordoma cell lines were evaluated in comparison with the control groups. For this purpose, it was aimed to determine biological markers that may be effective in chordoma. By processing the raw data, functional analysis of the genes allowed for a more comprehensive assessment of the pathways in addition to analyzing the most altered genes. The basis of the WikiPathways tool is the computation of the probability that changes in gene expression affect the number of genes in the pathway [96]. Using the WikiPathways tool, the pathways that exhibit significant differences as a consequence of IL-6R silencing were analyzed. According to WikiPathways analysis, common pathways were found in both cell lines. Among these, the VEGFA-VEGFR2 signaling pathway, the PI3K-Akt-mTOR signaling pathway, the focal adhesion pathway, and the MAPK signaling pathway are some

of the prominent pathways associated with cancer. The VEGFA-VEGFR2 signaling pathway promotes malignant transformation as well as cell proliferation, migration, and survival by regulating neo-angiogenesis [33, 126]. The PI3K/Akt/mTOR pathway is known to be active in a variety of cancer types including sarcomas, through processes including cell growth, cell division, and apoptotic escape [10, 127, 128]. Williams et al. reported similar activation in chordomas, suggesting a crucial role for this pathway in the pathophysiology of chordomas [129]. These pathways are assumed to reflect the aggressive potential of chordoma, as they are altered in shIL-6R groups.

According to the KEGG pathway analysis of the DAVID database, the Hippo signaling pathway was found to be significantly increased in both cell lines. The Hippo signaling pathway, whose dysregulation promotes cancer development, is an evolutionarily conserved pathway that keeps organ size under control by regulating cell proliferation, apoptosis, homeostasis, and self-renewal mechanisms [130, 131]. Studies have demonstrated in the literature that STAT3 activity is suppressed by the Hippo pathway [132]. This is consistent with increased Hippo signaling upon silencing of IL6R, which correlated with altered STAT3 expression in our project. The extracellular signals and membrane receptors controlling the Hippo pathway remain poorly known, despite a decade of intensive research on the mechanism [133]. The mechanisms of action of Hippo pathway implicate that it is essential for the process of carcinogenesis. This pathway, which is not yet fully understood, should be the focus of future research on chordoma.

In this study, 2 terms were identified in the GO terms tool that showed significant changes in both cell lines following IL-6R silencing. These are the Golgi membrane and nucleus, which are parts of the cellular component set and show a significant decrease in expression. Due to IL-6R suppression and lower expression of the genes encoding this function in the Golgi, this may point to a reduction in IL-6-induced Golgi trafficking in cells [134]. Furthermore, the transcriptomic changes that occur in cells after IL-6R silencing directly affect transcription in the nucleus, making it possible to include the term nucleus in the analysis [135, 136].

According to the transcriptomic findings, some of the genes whose expression changed significantly and increased/decreased the most according to fold difference are listed (Table 4.2). In the generation of the listed genes, it was important to select genes in the coding or multi-complex gene category. Among the genes with the highest or lowest fold change in

differential expression, there were no common genes for the chordoma cell lines used in this study. This may be due to the difference in primary/relapse status between the cell lines. In addition, genes that are listed for each cell line may also be chordoma targets. Interestingly, most of the genes on the list have been associated with different types of cancer in the literature but have not yet been discovered in chordoma.

The Ribonuclease A Family Member 2 (RNASE2) is an RNA-binding protein belonging to the pancreatic ribonuclease family. Moreover, the antiviral activity of RNASE2 has also been reported [137]. RNASE2 gene is known to be upregulated in AML, colorectal cancer, and other cancer types, especially gliomas [138–140]. In our study, its expression was significantly decreased in chordomas in which the IL-6R gene was silenced. The reversal of this effect by silencing the IL-6R gene in this study may be of critical importance for chordoma.

The PCSK2 (Proprotein Convertase Subtilisin/Kexin Type 2) is known to exhibit serine-type endopeptidase activity and has colocalization with the secretory granule. PCSK2 is essential for determining the initial site of the tumor and has been found to be a prognostic marker in a variety of cancer types [141–143]. The PCSK2 gene was one of six potential genes in a study that predicted the association between tumor immune cell infiltration and patient prognosis for esophageal squamous cell carcinoma [144]. In our study, this gene, which showed a significant decrease in IL-6R silenced groups, has the potential to be a target gene for chordoma.

In our study, GPNMB (glycoprotein non-metastatic/b) was another gene whose expression was significantly downregulated. This gene encodes a transmembrane glycoprotein. GPNMB is overexpressed in some malignant cells, such as osteosarcoma, and expressed in cells involved in the repair of tissues [145]. It has also been established in the literature that some cancer types are immunosuppressed by the GPNMB gene [146–148]. According to our research, the decreased expression of this gene in IL-6R silenced groups may be crucial for the immune cells' defense mechanism against chordoma.

The gene GPC4 (Glypican 4) has a significantly increased expression in our study. This gene encodes a cell surface proteoglycan carrying heparan sulfate. It is also listed among bone-related genes according to The Human Gene Database (Genecards). Based on an investigation, it has been demonstrated that downregulation of GPC4 facilitates breast,

pancreatic, and colorectal cancer progression by inducing cell migration and proliferation [149]. The literature-determined efficacy of GPC4 was reversed by IL-6R silencing, as demonstrated by the significant upregulation of this gene's expression in our study. Consequently, this gene may be a target for chordoma therapies.

PPDPF (Pancreatic Progenitor Cell Differentiation and Proliferation Factor), which has possible binding sites for PDZ, SH2, SH3, and GTP, is a significant regulator of exocrine pancreatic development. It was another gene whose expression was significantly higher in IL-6R-silenced groups. Although this gene's effects on cancer types are variable [150, 151]. Several studies have shown that the PPDPF gene inhibits the growth of hepatocellular carcinoma, which is consistent with our findings [152].

LDOC1, MAGEC2, HAPLN1, FOSL1, MATN2 genes are listed among top 10 DEGs that regulating IL-6R-associated chordoma carcinogenesis. These five genes associated with chordomas in the literature. The presence of these genes in the list indicates that their expression in the chordoma is associated with the IL-6R molecule.

6. CONCLUSION

The results of our study showed that knock down of IL-6 signaling induces transcriptional and functional changes in chordoma. Stable IL-6R gene-silenced chordoma cell lines have been established by the shRNA approach to achieve this. Experiments were carried out to assess the effects of IL-6R silencing on cellular function by evaluating the capacities of migration, invasion, scratch assay, and tumor-sphere formation. Furthermore, to determine the alteration in transcriptomic profile altered by IL-6R silencing, microarray experiments were conducted. The results showed that inhibition of IL-6R-mediated IL-6 signaling diminishes the aggressiveness-related genes and pathways in chordoma. The transcriptome effect of IL-6R inhibition in the study showed significant changes in certain crucial genes and pathways associated with cancer.

Target genes were selected among protein coding genes. Our research focused on genes that have not previously been investigated in chordoma but have been linked to other malignancies in the literature. These criteria led to the identification of RNASE2, PCSK2, GPNMB, GPC4 and PPDPF as target genes regulating IL-6R-associated chordoma carcinogenesis. The pathway analysis revealed a considerable increase in the Hippo signaling pathway in both cell lines, suggesting that this pathway is crucial for the chordoma-IL6 signaling interaction. To summarize the critical findings of our investigation:

The shRNA technique was successful in providing a stable efficacy for chordoma cell lines that are very difficult to transduce. For optimal efficiency, it was crucial to utilize plasmid options with different IL-6R target region sequences rather than only one shRNA plasmid choice.

After establishing stable cell lines, it has been found that using antibiotic selection alone is insufficient. Instead, fluorescent protein should be utilized to ensure cell separation.

In chordoma cell lines, it was found that IL-6R silencing reduce the functional aggressiveness (cell motility, migration/invasion ability). Further investigation is necessary considering the opposing findings obtained from the tumor-sphere forming assay.

Recombinant IL-6 did not substantially alter cellular function when included in the cell culture medium, except for the tumor-sphere formation assay.

The transcriptomic profile affected by IL-6R silencing showed that the Hippo signaling pathway was altered in both cell lines.

Transcriptomic analysis demonstrated that the RNASE2, PCSK2, GPNMB, GPC4, and PPDPF genes are potential candidates for IL-6 signaling in chordoma.

The results confirm preliminary studies and show that IL-6 signaling contributes to chordoma aggressiveness.

Part of this study was supported by the Scientific and Technological Research Council of Turkey [Grant number 222S197].

REFERENCES

1. Fu T, Dai L-J, Wu S-Y, et al. Spatial architecture of the immune microenvironment orchestrates tumor immunity and therapeutic response. *Journal of Hematology & Oncology* 2021; 14: 98.

2. Chen L, Oke T, Siegel N, et al. The Immunosuppressive Niche of Soft-Tissue Sarcomas is Sustained by Tumor-Associated Macrophages and Characterized by Intratumoral Tertiary Lymphoid Structures. *Clin Cancer Res* 2020; 26: 4018–4030.

3. Nagl S, Haas M, Lahmer G, et al. Cell-to-cell distances between tumor-infiltrating inflammatory cells have the potential to distinguish functionally active from suppressed inflammatory cells. *Oncoimmunology* 2016; 5: e1127494.

4. Gartrell RD, Marks DK, Hart TD, et al. Quantitative Analysis of Immune Infiltrates in Primary Melanoma. *Cancer Immunol Res* 2018; 6: 481–493.

5. Li Y, Dong B, Yuan P. The diagnostic value of machine learning for the classification of malignant bone tumor: a systematic evaluation and meta-analysis. *Front Oncol* 2023; 13: 1207175.

6. Weber K, Damron TA, Frassica FJ, et al. Malignant bone tumors. *Instr Course Lect* 2008; 57: 673–688.

7. Ulici V, Hart J. Chordoma: A Review and Differential Diagnosis. *Archives of Pathology & Laboratory Medicine* 2021; 146: 386–395.

8. Fletcher CDM, Unni K, Mertens F. *World Health Organization Classification of Tumours. Pathology and Genetics of Tumours of Soft Tissue and Bone*. IARC Press; 2002.

9. Crapanzano JP, Ali SZ, Ginsberg MS, et al. Chordoma: a cytologic study with histologic and radiologic correlation. *Cancer* 2001; 93: 40–51.

10. Lebellec L, Chauffert B, Blay J-Y, et al. Advanced chordoma treated by first-line molecular targeted therapies: Outcomes and prognostic factors. A retrospective study of the French Sarcoma Group (GSF/GETO) and the Association des Neuro-

Oncologues d'Expression Française (ANOCEF). *Eur J Cancer* 2017; 79: 119–128.

11. Ma T, Bai J, Zhang Y. Current understanding of brachyury in chordoma. *Biochimica et Biophysica Acta (BBA) - Reviews on Cancer* 2023; 1878: 189010.

12. Hsu W, Mohyeldin A, Shah SR, et al. Generation of chordoma cell line JHC7 and the identification of Brachyury as a novel molecular target: Laboratory investigation. *Journal of Neurosurgery* 2011; 115: 760–769.

13. Dridi M, Boutonnat J, Dumollard JM, et al. Patterns of brachyury expression in chordomas. *Annals of Diagnostic Pathology* 2021; 53: 151760.

14. Li L, Yu R, Cai T, et al. Effects of immune cells and cytokines on inflammation and immunosuppression in the tumor microenvironment. *International Immunopharmacology* 2020; 88: 106939.

15. Anderson NM, Simon MC. The tumor microenvironment. *Curr Biol* 2020; 30: R921–R925.

16. Shiao SL, Coussens LM. The Tumor-Immune Microenvironment and Response to Radiation Therapy. *J Mammary Gland Biol Neoplasia* 2010; 15: 411–421.

17. Lv B, Wang Y, Ma D, et al. Immunotherapy: Reshape the Tumor Immune Microenvironment. *Front Immunol* 2022; 13: 844142.

18. Deepak KGK, Vempati R, Nagaraju GP, et al. Tumor microenvironment: Challenges and opportunities in targeting metastasis of triple negative breast cancer. *Pharmacological Research* 2020; 153: 104683.

19. Fidler IJ, Poste G. The "seed and soil" hypothesis revisited. *The Lancet Oncology* 2008; 9: 808.

20. Paget S. THE DISTRIBUTION OF SECONDARY GROWTHS IN CANCER OF THE BREAST. *The Lancet* 1889; 133: 571–573.

21. Hass R, von der Ohe J, Ungefroren H. The Intimate Relationship among EMT, MET and TME: A T(ransdifferentiation) E(nhancing) M(ix) to Be Exploited for Therapeutic Purposes. *Cancers* 2020; 12: 3674.

22. Aggarwal V, Montoya CA, Donnenberg VS, et al. Interplay between tumor microenvironment and partial EMT as the driver of tumor progression. *iScience* 2021; 24: 102113.

23. Brabletz S, Schuhwerk H, Brabletz T, et al. Dynamic EMT: a multi-tool for tumor progression. *The EMBO Journal* 2021; 40: e108647.

24. Zheng X, Yu C, Xu M. Linking Tumor Microenvironment to Plasticity of Cancer Stem Cells: Mechanisms and Application in Cancer Therapy. *Front Oncol* 2021; 11: 678333.

25. Li Y-R, Fang Y, Lyu Z, et al. Exploring the dynamic interplay between cancer stem cells and the tumor microenvironment: implications for novel therapeutic strategies. *J Transl Med* 2023; 21: 686.

26. Binnewies M, Roberts EW, Kersten K, et al. Understanding the tumor immune microenvironment (TIME) for effective therapy. *Nat Med* 2018; 24: 541–550.

27. Rous P, Murphy JB. THE HISTOLOGICAL SIGNS OF RESISTANCE TO A TRANSMISSIBLE SARCOMA OF THE FOWL. *J Exp Med* 1912; 15: 270–286.

28. Lippitz BE. Cytokine patterns in patients with cancer: a systematic review. *The Lancet Oncology* 2013; 14: e218–e228.

29. Waldmann TA. Cytokines in Cancer Immunotherapy. *Cold Spring Harb Perspect Biol* 2018; 10: a028472.

30. Conlon KC, Miljkovic MD, Waldmann TA. Cytokines in the Treatment of Cancer. *Journal of Interferon & Cytokine Research* 2019; 39: 6–21.

31. Virchow R. *Cellular Pathology as Based Upon Physiological and Pathological Histology* ... J.B. Lippincott, 1863.

32. Waldmann TA, Chen J. Disorders of the JAK/STAT Pathway in T Cell Lymphoma Pathogenesis: Implications for Immunotherapy. *Annual Review of Immunology* 2017; 35: 533–550.

33. Hanahan D, Weinberg RA. Hallmarks of Cancer: The Next Generation. *Cell* 2011;

144: 646–674.

34. Coussens LM, Werb Z. Inflammation and cancer. *Nature* 2002; 420: 860–867.

35. Khandia R, Munjal A. Interplay between inflammation and cancer. *Advances in Protein Chemistry and Structural Biology*. 2020:199–245.

36. Bilgic MB, Yengin GI, Bayrak OF. Cytokines and Cancer. *Autoimmunity and Cancer*. 2022:217-239.

37. Propper DJ, Balkwill FR. Harnessing cytokines and chemokines for cancer therapy. *Nat Rev Clin Oncol* 2022; 19: 237–253.

38. Choy EH, De Benedetti F, Takeuchi T, et al. Translating IL-6 biology into effective treatments. *Nat Rev Rheumatol* 2020; 16: 335–345.

39. Kang S, Kishimoto T. Interplay between interleukin-6 signaling and the vascular endothelium in cytokine storms. *Exp Mol Med* 2021; 53: 1116–1123.

40. Uciechowski P, Dempke WCM. Interleukin-6: A Masterplayer in the Cytokine Network. *Oncology* 2020; 98: 131–137.

41. Rose-John S, Winthrop K, Calabrese L. The role of IL-6 in host defence against infections: immunobiology and clinical implications. *Nat Rev Rheumatol* 2017; 13: 399–409.

42. Hunter CA, Jones SA. IL-6 as a keystone cytokine in health and disease. *Nat Immunol* 2015; 16: 448–457.

43. Calabrese LH, Rose-John S. IL-6 biology: implications for clinical targeting in rheumatic disease. *Nat Rev Rheumatol* 2014; 10: 720–727.

44. Schiff MH, Kremer JM, Jahreis A, et al. Integrated safety in tocilizumab clinical trials. *Arthritis Research & Therapy* 2011; 13: R141.

45. Manore SG, Doheny DL, Wong GL, et al. IL-6/JAK/STAT3 Signaling in Breast Cancer Metastasis: Biology and Treatment. *Front Oncol* 2022; 12: 866014.

46. Tobin RP, Jordan KR, Kapoor P, et al. IL-6 and IL-8 Are Linked With Myeloid-Derived Suppressor Cell Accumulation and Correlate With Poor Clinical Outcomes in Melanoma Patients. *Front Oncol* 2019; 9: 1223.

47. Xu J, Lin H, Wu G, et al. IL-6/STAT3 Is a Promising Therapeutic Target for Hepatocellular Carcinoma. *Front Oncol* 2021; 11: 760971.

48. Weber JS, Tang H, Hippeli L, et al. Serum IL-6 and CRP as prognostic factors in melanoma patients receiving single agent and combination checkpoint inhibition. *JCO* 2019; 37: 100–100.

49. Rhee F van, Wong RS, Munshi N, et al. Siltuximab for multicentric Castleman's disease: a randomised, double-blind, placebo-controlled trial. *The Lancet Oncology* 2014; 15: 966–974.

50. Janahiraman S, Too CL, Lee KW, et al. Genetic Biomarkers as Predictors of Response to Tocilizumab in Rheumatoid Arthritis: A Systematic Review and Meta-Analysis. *Genes* 2022; 13: 1284.

51. Sainz L, Riera P, Moya P, et al. Role of IL6R Genetic Variants in Predicting Response to Tocilizumab in Patients with Rheumatoid Arthritis. *Pharmaceutics* 2022; 14: 1942.

52. Nouri B, Nair N, Barton A. Predicting treatment response to IL6R blockers in rheumatoid arthritis. *Rheumatology* 2020; 59: 3603–3610.

53. Expression of Concern: Fingolimod inhibits proliferation and epithelial–mesenchymal transition in sacral chordoma by inactivating IL-6/STAT3 signaling. *Bioscience Reports* 2020; 40: BSR-20200221_EOC.

54. Gulluoglu S, Tuysuz EC, Sahin M, et al. The role of TNF-α in chordoma progression and inflammatory pathways. *Cell Oncol* 2019; 42: 663–677.

55. Xu J, Shi Q, Lou J, et al. Chordoma recruits and polarizes tumor-associated macrophages via secreting CCL5 to promote malignant progression. *J Immunother Cancer* 2023; 11: e006808.

56. Redman M, King A, Watson C, et al. What is CRISPR/Cas9? *Arch Dis Child Educ Pract Ed* 2016; 101: 213–215.

57. Ran FA, Hsu PD, Wright J, et al. Genome engineering using the CRISPR-Cas9 system. *Nat Protoc* 2013; 8: 2281–2308.

58. Duckert B, Fauvart M, Goos P, et al. High-definition electroporation: Precise and efficient transfection on a microelectrode array. *J Control Release* 2022; 352: 61–73.

59. Kumar P, Nagarajan A, Uchil PD. Electroporation. *Cold Spring Harb Protoc*; 2019.

60. Potter H, Heller R. Transfection by Electroporation. *Curr Protoc Immunol* 2017; 117: 10.15.1-10.15.9.

61. Aluigi M, Fogli M, Curti A, et al. Nucleofection Is an Efficient Nonviral Transfection Technique for Human Bone Marrow–Derived Mesenchymal Stem Cells. *Stem Cells* 2006; 24: 454–461.

62. Distler JHW, Jüngel A, Kurowska-Stolarska M, et al. Nucleofection: a new, highly efficient transfection method for primary human keratinocytes*. *Exp Dermatol* 2005; 14: 315–320.

63. Fong H, Elliott KAH, Lock LF, et al. Nucleofection of human embryonic stem cells. *Methods Mol Biol* 2011; 767: 333–341.

64. Majtnerová P, Roušar T. An overview of apoptosis assays detecting DNA fragmentation. *Mol Biol Rep* 2018; 45: 1469–1478.

65. Matassov D, Kagan T, Leblanc J, et al. Measurement of apoptosis by DNA fragmentation. Methods Mol Biol 2004; 282: 1–17.

66. Rahbar Saadat Y, Saeidi N, Zununi Vahed S, et al. An update to DNA ladder assay for apoptosis detection. *Bioimpacts* 2015; 5: 25–28.

67. Zhang JH, Xu M. DNA fragmentation in apoptosis. *Cell Res* 2000; 10: 205–211.

68. Siolas D, Lerner C, Burchard J, et al. Synthetic shRNAs as potent RNAi triggers.

Nat Biotechnol 2005; 23: 227–231.

69. Becker J, Fischer N, Grimm D. Right on target: The next class of efficient, safe, and specific RNAi triggers. *Molecular Therapy - Nucleic Acids* 2022; 28: 363–365.

70. Al-Jomah N, Al-Mohanna FH, Aboussekhra A. Tocilizumab suppresses the pro-carcinogenic effects of breast cancer-associated fibroblasts through inhibition of the STAT3/AUF1 pathway. *Carcinogenesis* 2021; 42: 1439–1448.

71. Méndez-Clemente A, Bravo-Cuellar A, González-Ochoa S, et al. Dual STAT-3 and IL-6R inhibition with stattic and tocilizumab decreases migration, invasion and proliferation of prostate cancer cells by targeting the IL-6/IL-6R/STAT-3 axis. *Oncol Rep* 2022; 48: 138.

72. Sainz L, Riera P, Moya P, et al. Role of IL6R Genetic Variants in Predicting Response to Tocilizumab in Patients with Rheumatoid Arthritis. *Pharmaceutics* 2022; 14: 1942.

73. Bahmad HF, Cheaito K, Chalhoub RM, et al. Sphere-Formation Assay: Three-Dimensional in vitro Culturing of Prostate Cancer Stem/Progenitor Sphere-Forming Cells. *Front Oncol* 2018; 8: 347.

74. Wang H, Paczulla AM, Konantz M, et al. In Vitro Tumorigenic Assay: The Tumor Spheres Assay. *Methods Mol Biol* 2018; 1692: 77–87.

75. Yoshida K, Taga T, Saito M, et al. Targeted disruption of gp130, a common signal transducer for the interleukin 6 family of cytokines, leads to myocardial and hematological disorders. *Proceedings of the National Academy of Sciences* 1996; 93: 407–411.

76. Zhu Y, Ma N, Li H-X, et al. Berberine induces apoptosis and DNA damage in MG-63 human osteosarcoma cells. *Molecular Medicine Reports* 2014; 10: 1734–1738.

77. Yon Rhee S, Wood V, Dolinski K, et al. Use and misuse of the gene ontology annotations. *Nat Rev Genet* 2008; 9: 509–515.

78. HEINRICH PC, BEHRMANN I, MÜLLER-NEWEN G, et al. Interleukin-6-type

cytokine signalling through the gp130/Jak/STAT pathway1. *Biochemical Journal* 1998; 334: 297–314.

79. Kamimura D, Ishihara K, Hirano T. IL-6 signal transduction and its physiological roles: the signal orchestration model. *Rev Physiol Biochem Pharmacol* 2003; 149: 1–38.

80. Jones SA, Scheller J, Rose-John S. Therapeutic strategies for the clinical blockade of IL-6/gp130 signaling. *J Clin Invest* 2011; 121: 3375–3383.

81. Ma M, Sun Q, Li X, et al. Blockade of IL-6/IL-6R Signaling Attenuates Acute Antibody-Mediated Rejection in a Mouse Cardiac Transplantation Model. *Front Immunol* 2021; 12: 778359.

82. McFarland-Mancini MM, Funk HM, Paluch AM, et al. Differences in wound healing in mice with deficiency of IL-6 versus IL-6 receptor. *J Immunol* 2010; 184: 7219–7228.

83. Horváth BV, Falus A, Tóth S, et al. Inverse regulation of interleukin-6 (IL-6) and IL-6 receptor in histamine deficient histidine decarboxylase-knock-out mice. *Immunology Letters* 2002; 80: 151–154.

84. Wong KA, Harker JA, Dolgoter A, et al. T Cell-Intrinsic IL-6R Signaling Is Required for Optimal ICOS Expression and Viral Control during Chronic Infection. *J Immunol* 2019; 203: 1509–1520.

85. Tanaka T, Kishimoto T. Targeting interleukin-6: all the way to treat autoimmune and inflammatory diseases. *Int J Biol Sci* 2012; 8: 1227–1236.

86. Motegi Y, Katayama K, Sakurai F, et al. An effective gene-knockdown using multiple shRNA-expressing adenovirus vectors. *Journal of Controlled Release* 2011; 153: 149–153.

87. Lan S-H, Lai C-C, Huang H-T, et al. Tocilizumab for severe COVID-19: a systematic review and meta-analysis. *International Journal of Antimicrobial Agents* 2020; 56: 106103.

88. Chung AW, Kozielski AJ, Qian W, et al. Tocilizumab overcomes chemotherapy resistance in mesenchymal stem-like breast cancer by negating autocrine IL-1A induction of IL-6. *NPJ Breast Cancer* 2022; 8: 30.

89. Venkiteshwaran A. Tocilizumab. *mAbs* 2009; 1: 432–438.

90. Prenissl N, Lokau J, Rose-John S, et al. Therapeutic blockade of the interleukin-6 receptor (IL-6R) allows sIL-6R generation by proteolytic cleavage. *Cytokine* 2019; 114: 1–5.

91. Wang X, Lee SO, Xia S, et al. Endothelial Cells Enhance Prostate Cancer Metastasis via IL-6→Androgen Receptor→TGF-β→MMP-9 Signals. *Molecular Cancer Therapeutics* 2013; 12: 1026–1037.

92. Rašková M, Lacina L, Kejík Z, et al. The Role of IL-6 in Cancer Cell Invasiveness and Metastasis—Overview and Therapeutic Opportunities. *Cells* 2022; 11: 3698.

93. Rinner B, Froehlich EV, Buerger K, et al. Establishment and detailed functional and molecular genetic characterisation of a novel sacral chordoma cell line, MUG-Chor1. *International Journal of Oncology* 2012; 40: 443–451.

94. Fuster JJ, Walsh K. The Good, the Bad, and the Ugly of interleukin-6 signaling. *The EMBO Journal* 2014; 33: 1425–1427.

95. Park J-I, Lee M-G, Cho K, et al. Transforming growth factor-β1 activates interleukin-6 expression in prostate cancer cells through the synergistic collaboration of the Smad2, p38-NF-κB, JNK, and Ras signaling pathways. *Oncogene* 2003; 22: 4314–4332.

96. Zhou B, Wang J, Zhao B. Micromorphology characterization and reconstruction of sand particles using micro X-ray tomography and spherical harmonics. *Engineering Geology* 2015; 184: 126–137.

97. Gulluoglu S, Turksoy O, Kuskucu A, et al. The molecular aspects of chordoma. *Neurosurg Rev* 2016; 39: 185–196.

98. Li J, Shen J, Wang K, et al. The Roles of Sox Family Genes in Sarcoma. *Current*

Drug Targets 2016; 17: 1761–1772.

99. Chico, MA, Mesas, C, et al. Cancer Stem Cells in Sarcomas: In Vitro Isolation and Role as Prognostic Markers. *Cancers* 2023; 15: 2449.

100. Das B, Pal B, Bhuyan R, et al. MYC Regulates the HIF2α Stemness Pathway via Nanog and Sox2 to Maintain Self-Renewal in Cancer Stem Cells versus Non-Stem Cancer Cells. *Cancer Research* 2019; 79: 4015–4025.

101. Roudi R, Barodabi M, Madjd Z, et al. Expression patterns and clinical significance of the potential cancer stem cell markers OCT4 and NANOG in colorectal cancer patients. *Molecular & Cellular Oncology* 2020; 7: 1788366.

102. Alemohammad H, Asadzadeh Z, Motafakker Azad R, et al. Signaling pathways and microRNAs, the orchestrators of NANOG activity during cancer induction. *Life Sci* 2020; 260: 118337.

103. Najafzadeh B, Asadzadeh Z, Motafakker Azad R, et al. The oncogenic potential of NANOG: An important cancer induction mediator. *J Cell Physiol* 2021; 236: 2443–2458.

104. Yoon C, Lu J, Yi BC, et al. PI3K/Akt pathway and Nanog maintain cancer stem cells in sarcomas. *Oncogenesis* 2021; 10: 12.

105. Guo Y, Liu S, Wang P, et al. Expression profile of embryonic stem cell-associated genes Oct4, Sox2 and Nanog in human gliomas. *Histopathology* 2011; 59: 763–775.

106. Asadi MH, Mowla SJ, Fathi F, et al. OCT4B1, a novel spliced variant of OCT4, is highly expressed in gastric cancer and acts as an antiapoptotic factor. *Int J Cancer* 2011; 128: 2645–2652.

107. Iida H, Suzuki M, Goitsuka R, et al. Hypoxia induces CD133 expression in human lung cancer cells by up-regulation of OCT3/4 and SOX2. *Int J Oncol* 2012; 40: 71–79.

108. Dai X, Ge J, Wang X, et al. OCT4 regulates epithelial-mesenchymal transition and its knockdown inhibits colorectal cancer cell migration and invasion. *Oncology*

Reports 2013; 29: 155–160.

109. Novak D, Hüser L, Elton JJ, et al. SOX2 in development and cancer biology. *Seminars in Cancer Biology* 2020; 67: 74–82.

110. Schaefer T, Lengerke C. SOX2 protein biochemistry in stemness, reprogramming, and cancer: the PI3K/AKT/SOX2 axis and beyond. *Oncogene* 2020; 39: 278–292.

111. Zhang S, Xiong X, Sun Y. Functional characterization of SOX2 as an anticancer target. *Sig Transduct Target Ther* 2020; 5: 1–17.

112. Tuysuz EC, Gulluoglu S, Yaltirik CK, et al. Distinctive role of dysregulated miRNAs in chordoma cancer stem-like cell maintenance. *Experimental Cell Research* 2019; 380: 9–19.

113. Zeisberg M, Neilson EG. Biomarkers for epithelial-mesenchymal transitions. *J Clin Invest* 2009; 119: 1429–1437.

114. Banyard J, Bielenberg DR. The role of EMT and MET in cancer dissemination. *Connect Tissue Res* 2015; 56: 403–413.

115. Rokavec M, Öner MG, Li H, et al. IL-6R/STAT3/miR-34a feedback loop promotes EMT-mediated colorectal cancer invasion and metastasis. *J Clin Invest* 2014; 124: 1853–1867.

116. Parker J, Hockney S, Blaschuk OW, et al. Targeting N-cadherin (CDH2) and the malignant bone marrow microenvironment in acute leukaemia. *Expert Reviews in Molecular Medicine* 2023; 25: e16.

117. Zhang C. Role of cadherin 2 in intervertebral disc maturation. PhD Thesis, University of Hong Kong, 2018.

118. van Roy F. Beyond E-cadherin: roles of other cadherin superfamily members in cancer. *Nat Rev Cancer* 2014; 14: 121–134.

119. Yuan W, Wei F, Ouyang H, et al. CMTM3 suppresses chordoma progress through EGFR/STAT3 regulated EMT and TP53 signaling pathway. *Cancer Cell Int* 2021; 21: 510.

120. Satelli A, Li S. Vimentin in cancer and its potential as a molecular target for cancer therapy. *Cell Mol Life Sci* 2011; 68: 3033–3046.

121. Huo Y, Zheng Z, Chen Y, et al. Downregulation of vimentin expression increased drug resistance in ovarian cancer cells. *Oncotarget* 2016; 7: 45876–45888.

122. Du L, Li J, Lei L, et al. High Vimentin Expression Predicts a Poor Prognosis and Progression in Colorectal Cancer: A Study with Meta-Analysis and TCGA Database. *Biomed Res Int* 2018; 2018: 6387810.

123. Liu S, Liu L, Ye W, et al. High Vimentin Expression Associated with Lymph Node Metastasis and Predicated a Poor Prognosis in Oral Squamous Cell Carcinoma. *Sci Rep* 2016; 6: 38834.

124. Szubert S, Koper K, Dutsch-Wicherek MM, et al. High tumor cell vimentin expression indicates prolonged survival in patients with ovarian malignant tumors. *Ginekol Pol* 2019; 90: 11–19.

125. Zhao J, Zhang L, Dong X, et al. High Expression of Vimentin is Associated With Progression and a Poor Outcome in Glioblastoma. *Appl Immunohistochem Mol Morphol* 2018; 26: 337–344.

126. Koch S, Claesson-Welsh L. Signal transduction by vascular endothelial growth factor receptors. *Cold Spring Harb Perspect Med* 2012; 2: a006502.

127. Stacchiotti S, Van Tine BA. Synovial Sarcoma: Current Concepts and Future Perspectives. *JCO* 2018; 36: 180–187.

128. Wang L, Zehir A, Nafa K, et al. Genomic aberrations frequently alter chromatin regulatory genes in chordoma. *Genes Chromosomes Cancer* 2016; 55: 591–600.

129. Williams BJ, Raper DMS, Godbout E, et al. Diagnosis and Treatment of Chordoma. *Journal of the National Comprehensive Cancer Network* 2013; 11: 726–731.

130. Pan D. The hippo signaling pathway in development and cancer. *Dev Cell* 2010; 19: 491–505.

131. Zhao B, Tumaneng K, Guan K-L. The Hippo pathway in organ size control, tissue

regeneration and stem cell self-renewal. *Nat Cell Biol* 2011; 13: 877–883.

132. Tang Q, Fang J, Lai W, et al. Hippo pathway monomerizes STAT3 to regulate prostate cancer growth. *Cancer Sci* 2022; 113: 2753–2762.

133. Fu M, Hu Y, Lan T, et al. The Hippo signalling pathway and its implications in human health and diseases. *Signal Transduct Target Ther* 2022; 7: 376.

134. Verboogen DRJ, Revelo NH, ter Beest M, et al. Interleukin-6 secretion is limited by self-signaling in endosomes. *Journal of Molecular Cell Biology* 2019; 11: 144–157.

135. Goler-Baron V, Selitrennik M, Barkai O, et al. Transcription in the nucleus and mRNA decay in the cytoplasm are coupled processes. *Genes Dev* 2008; 22: 2022–2027.

136. Karin M. Signal transduction from the cell surface to the nucleus through the phosphorylation of transcription factors. *Current Opinion in Cell Biology* 1994; 6: 415–424.

137. Lu L, Li J, Wei R, et al. Selective cleavage of ncRNA and antiviral activity by RNase2/EDN in THP1-induced macrophages. *Cell Mol Life Sci* 2022; 79: 209.

138. Niu W, He H. RNASE2 is a prognostic biomarker and is correlated with immune infiltration in glioma. *Research Square*; 2022.

139. Yu M, Zhang Y, Mao R, et al. A Risk Model of Eight Immune-Related Genes Predicting Prognostic Response to Immune Therapies for Gastric Cancer. *Genes (Basel)* 2022; 13: 720.

140. Xiang Y, Zhou S, Hao J, et al. Development and validation of a prognostic model for kidney renal clear cell carcinoma based on RNA binding protein expression. *Aging (Albany NY)* 2020; 12: 25356–25372.

141. Cai C, Zhang H, Zhu Y, et al. Serum Exosomal Long Noncoding RNA pcsk2-2:1 As A Potential Novel Diagnostic Biomarker For Gastric Cancer. *Onco Targets Ther* 2019; 12: 10035–10041.

142. Guo C, Zeng F, Liu H, et al. Establish immune-related gene prognostic index for

esophageal cancer. *Front Genet* 2022; 13: 956915.

143. Remes SM, Leijon H, Vesterinen T, et al. PCSK2 expression in neuroendocrine tumors points to a midgut, pulmonary, or pheochromocytoma-paraganglioma origin. *APMIS* 2020; 128: 563–572.

144. Ma C, Luo H. A more novel and robust gene signature predicts outcome in patients with esophageal squamous cell carcinoma. *Clin Res Hepatol Gastroenterol* 2022; 46: 102033.

145. Nakano K. Challenges of Systemic Therapy Investigations for Bone Sarcomas. *Int J Mol Sci* 2022; 23: 3540.

146. Lazaratos A-M, Annis MG, Siegel PM. GPNMB: a potent inducer of immunosuppression in cancer. *Oncogene* 2022; 41: 4573–4590.

147. Maric G, Annis MG, MacDonald PA, et al. GPNMB augments Wnt-1 mediated breast tumor initiation and growth by enhancing PI3K/AKT/mTOR pathway signaling and β-catenin activity. *Oncogene* 2019; 38: 5294–5307.

148. Son S, Kim H, Lim H, et al. CCN3/NOV promotes metastasis and tumor progression via GPNMB-induced EGFR activation in triple-negative breast cancer. *Cell Death Dis* 2023; 14: 81.

149. Munir J, Van Ngu T, Na Ayudthaya PD, et al. Downregulation of glypican-4 facilitates breast cancer progression by inducing cell migration and proliferation. *Biochem Biophys Res Commun* 2020; 526: 91–97.

150. Zi Y, Liu L, Gao J, et al. Phosphorylation of PPDPF via IL6-JAK2 activates the Wnt/β-catenin pathway in colorectal cancer. *EMBO reports* 2023; 24: e55060.

151. Zheng Q-W, Ni Q-Z, Zhu B, et al. PPDPF promotes lung adenocarcinoma progression via inhibiting apoptosis and NK cell-mediated cytotoxicity through STAT3. *Oncogene* 2022; 41: 4244–4256.

152. Wang Y-K, Ma N, Xu S, et al. PPDPF suppresses the development of hepatocellular carcinoma through TRIM21-mediated ubiquitination of RIPK1. *Cell Rep* 2023; 42:

112340.